Contribution from the Departments of Chemistry, Cornell University, Ithaca, New York 14853, and The University of Michigan, Ann Arbor, Michigan 48109

# Five-Coordinate Bent Metallocenes. Structure and Dynamics of Bis(η-cyclopentadienyl)chloro(*N*,*N*-dialkyldithiocarbamato)zirconium(IV) Complexes

MICHAEL E. SILVER,[1a] ODILE EISENSTEIN,*[1b] and ROBERT C. FAY*[1a]

*Received August 31, 1982*

The crystal and molecular structure of bis(η-cyclopentadienyl)chloro(*N*,*N*-diethyldithiocarbamato)zirconium(IV), $(\eta\text{-}C_5H_5)_2ZrCl[S_2CN(C_2H_5)_2]$, has been determined by X-ray diffraction and has been refined anisotropically by least-squares methods to $R_1 = 0.038$ and $R_2 = 0.048$ using 2048 independent diffractometer data having $2\theta_{\mathrm{Mo}\,K\alpha} \le 45.0°$ and $|F_o| > 2.0\sigma_F$. The compound crystallizes in the monoclinic space group $P2_1/n$ with four molecules in a cell having dimensions $a = 17.619\ (4)$ Å, $b = 13.892\ (3)$ Å, $c = 7.102\ (1)$ Å, and $\beta = 93.33\ (2)°$ ($\rho_{\mathrm{obsd}} = 1.549$, $\rho_{\mathrm{calcd}} = 1.551$ g cm$^{-3}$). The molecules have a five-coordinate bent metallocene structure with the Zr atom, Cl atom, and the two S atoms of the bidentate dithiocarbamate ligand lying in a quasi mirror plane that is nearly perpendicular to the plane defined by the Zr atom and the centroids of the two symmetrically attached $\eta\text{-}C_5H_5$ groups. Because of crowding in the $ZrClS_2C_{10}$ coordination group, the Zr–Cl and Zr–S bonds to the lateral coordination sites are unusually long (2.556 (2) and 2.723 (2) Å, respectively); these distances are the longest terminal Zr–Cl and Zr–S bond lengths yet observed for any structure involving Zr(IV). A 300-MHz $^1$H NMR study has yielded the following kinetic data for methyl group exchange in the corresponding *N*,*N*-dimethyl derivative, $(\eta\text{-}C_5H_5)_2ZrCl[S_2CN(CH_3)_2]$: $k(25\ °C) = 8.6$ s$^{-1}$, $\Delta G^*(25\ °C) = 16.18 \pm 0.08$ kcal/mol, $\Delta H^* = 15.9 \pm 2.0$ kcal/mol, $\Delta S^* = -1.0 \pm 6.8$ eu. Possible mechanisms for the exchange process have been analyzed on the basis of kinetic and structural data and extended Hückel molecular orbital calculations. A mechanism involving C$\overset{\dots}{-}$N bond rotation is preferred.

## Introduction

The electronic structure and molecular geometry[2-6] and the chemistry[7-13] of bent bis(η-cyclopentadienyl) transition metal complexes $(\eta\text{-}C_5H_5)_2ML_n$ are subjects of considerable current interest. These compounds exhibit a rich and novel chemistry. For example, bent metallocenes of group 4 transition metals have been shown to fix nitrogen,[7] functionalize olefins (hydrozirconation),[8] insert carbon monoxide into metal–carbon bonds,[9-11] reduce carbon monoxide under mild conditions,[12] and activate carbon dioxide.[13]

The vast majority of $(\eta\text{-}C_5H_5)_2M^{IV}$ complexes are 16-electron complexes with two additional ligands, $(\eta\text{-}C_5H_5)_2ML_2$.[14] Consequently, we have been interested in recent reports of the synthesis and characterization of a series of chloro–dithiocarbamato complexes of the type $(\eta\text{-}C_5H_5)_2MCl(S_2CNR_2)$ (M = Ti, Zr; R = alkyl),[15,16] $(\eta\text{-}C_5H_5)_2MCl(S_2CNHR)$ (M = Ti, Zr; R = aryl),[17,18] and $(\eta\text{-}C_5H_4CH_3)_2TiCl(S_2CNHR)$ (R = aryl).[19] These compounds are monomeric nonelectrolytes in solution, and IR evidence points to a bidentate attachment of the dithiocarbamate ligands. A five-coordinate trigonal-bipyramidal structure with the two cyclopentadienyl ligands in axial positions (1) has been proposed[15-18] on the basis of a single cyclopentadienyl resonance[15-18] and a single dithiocarbamate alkyl resonance[15,16] in 60-MHz $^1$H NMR spectra at 30 °C. This geometry is unprecedented and is unlikely for steric reasons. The expected bend metallocene structure (2) is consistent with the observed NMR spectra if (1) the complexes are fluxional at 30 °C or (2) the alkyl resonances are unresolved at 60 MHz. Because 18-electron $(\eta\text{-}C_5H_5)_2ML_3$ complexes are uncommon for group 4 transition metals[14] and because five-coordinate zirconium(IV) is rare,[20] we have determined the X-ray crystal structure of a representative bis(η-cyclopentadienyl)chloro(dithiocarbamato)zirconium(IV) complex, $(\eta\text{-}C_5H_5)_2ZrCl[S_2CN(C_2H_5)_2]$. The only other $(\eta\text{-}C_5H_5)_2ZrL_3$ complex whose structure has been established by X-ray diffraction is $(\eta\text{-}C_5H_5)_2Zr(COCH_3)(CH_3)$ (3), a bent metallocene that con-

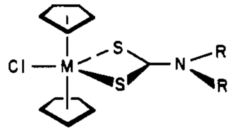

1

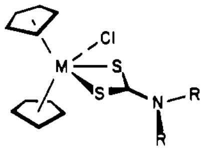

2

---

(1) (a) Cornell University. (b) The University of Michigan.

(2) Lauher, J. W.; Hoffman, R. *J. Am. Chem. Soc.* **1976**, *98*, 1729.

(3) Alcock, N. W. *J. Chem. Soc. A* **1967**, 2001.

(4) Green, J. C.; Green, M. L. H.; Prout, C. K. *J. Chem. Soc., Chem. Commun.* **1972**, 421.

(5) Prout, C. K.; Cameron, T. S.; Forder, R. A.; Critchley, S. R.; Denton, B.; Rees, G. V. *Acta Crystallogr., Sect. B* **1974**, *B30*, 2290.

(6) Petersen, J. L.; Dahl, L. F. *J. Am. Chem. Soc.* **1974**, *96*, 2248.

(7) (a) Bercaw, J. E. *J. Am. Chem. Soc.* **1974**, *96*, 5087. (b) Manriquez, J. M.; Bercaw, J. E. *Ibid.* **1974**, *96*, 6229.

(8) (a) Hart, D. W.; Schwartz, J. *J. Am. Chem. Soc.* **1974**, *96*, 8115. (b) Schwartz, J.; Labinger, J. A. *Angew. Chem., Int. Ed. Engl.* **1976**, *15*, 333.

(9) Bertelo, C. A.; Schwartz, J. *J. Am. Chem. Soc.* **1975**, *97*, 228.

(10) (a) Fachinetti, G.; Floriani, C.; Marchetti, F.; Merlino, S. *J. Chem. Soc., Chem. Commun.* **1976**, 522. (b) Fachinetti, G.; Fochi, G.; Floriani, C. *J. Chem. Soc., Dalton Trans.* **1977**, 1946.

(11) (a) Erker, G.; Rosenfeldt, F. *Angew. Chem., Int. Ed. Engl.* **1978**, *17*, 605. (b) Erker, G.; Rosenfeldt, F. *J. Organomet. Chem.* **1980**, *188*, C1.

(12) Wolczanski, P. T.; Bercaw, J. E. *Acc. Chem. Res.* **1980**, *13*, 121.

(13) Fachinetti, G.; Floriani, C.; Chiesi-Villa, A.; Guastini, C. *J. Am. Chem. Soc.* **1979**, *101*, 1767.

(14) Wailes, P. C.; Coutts, R. S. P.; Weigold, H. "Organometallic Chemistry of Titanium, Zirconium, and Hafnium"; Academic Press: New York, 1974.

(15) Jain, V. K.; Kumar, V.; Garg, B. S. *Inorg. Chim. Acta* **1978**, *26*, 197.

(16) Kaushik, N. K.; Bhushan, B.; Chhatwal, G. R. *Transition Met. Chem.* **1978**, *3*, 215.

(17) Kaushik, N. K.; Bhushan, B.; Chhatwal, G. R. *Synth. React. Inorg. Met.-Org. Chem.* **1978**, *8*, 467.

(18) Kaushik, N. K.; Bhushan, B.; Chhatwal, G. R. *J. Inorg. Nucl. Chem.* **1980**, *42*, 457.

(19) Kaushik, N. K.; Bhushan, B.; Chhatwal, G. R. *Z. Naturforsch., B: Anorg. Chem., Org. Chem.* **1979**, *34B*, 949.

(20) Cotton, F. A.; Wilkinson, G. "Advanced Inorganic Chemistry"; Wiley: New York, 1980.

0020-1669/83/1322-0759$01.50/0

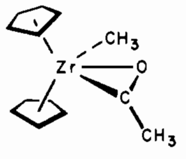

**3**

tains an $\eta^2$-acetyl ligand.[10] Very few ($\eta$-$C_5H_5$)$_2$$ML_3$ complexes of any type are known, perhaps due to the steric requirements of the three additional ligands. The best known examples are the trihydride complexes of group 5 and group 6 metallocenes, ($\eta$-$C_5H_5$)$_2$$NbH_3$,[21] ($\eta$-$C_5H_5$)$_2$$TaH_3$,[21,22] and [($\eta$-$C_5H_5$)$_2$$WH_3$]$^+$.[21,22]

The present work establishes the bent metallocene geometry 2 for ($\eta$-$C_5H_5$)$_2$ZrCl[$S_2CN(C_2H_5)_2$] and reveals some unusually long Zr–Cl and Zr–S bond distances. Also reported in this paper are (1) a variable-temperature NMR study of hindered rotation about the $C \overset{\cdots}{-} N$ bond in the dithiocarbamate ligand of ($\eta$-$C_5H_5$)$_2$ZrCl[$S_2CN(CH_3)_2$] and (2) extended Hückel molecular orbital calculations relating to the mechanism of metal-centered rearrangement in ($\eta$-$C_5H_5$)$_2$ZrCl($S_2CNR_2$) complexes.

## Experimental Section

**Reagents and General Techniques.** Sodium *N,N*-dimethyldithiocarbamate dihydrate, Na[$S_2CN(CH_3)_2$]·2$H_2O$, was prepared by reaction in aqueous solution of equimolar amounts of dimethylamine, carbon disulfide, and sodium hydroxide.[23] Na[$S_2CN(C_2H_5)_2$]·3$H_2O$ was obtained from Fisher Scientific Co. Both salts were dried in vacuo over phosphorus(V) oxide at 110 °C until their infrared spectra showed no water. Solvents were dried by refluxing for at least 24 h over phosphorus(V) oxide (dichloromethane and carbon tetrachloride) or calcium hydride (hexane). All syntheses and subsequent handling of the ($\eta$-$C_5H_5$)$_2$ZrCl($S_2CNR_2$) complexes were conducted under anhydrous conditions in a dry nitrogen atmosphere.

**Bis($\eta$-cyclopentadienyl)chloro(*N,N*-dimethyldithiocarbamato)zirconium(IV).** This compound was prepared by the method of Jain et al.[15] by reaction for 24 h of equimolar amounts of ($\eta$-$C_5H_5$)$_2$$ZrCl_2$ (Alfa Products) and anhydrous Na[$S_2CN(CH_3)_2$] in refluxing dichloromethane. Recrystallization from dichloromethane–hexane afforded clear, colorless crystals of ($\eta$-$C_5H_5$)$_2$ZrCl[$S_2CN(CH_3)_2$]; the solid decomposes without melting at 210–220 °C (lit.[15] mp 205–210 °C dec). Anal. Calcd for Zr($C_5H_5$)$_2$($C_3H_6NS_2$)Cl: C, 41.41; H, 4.28; Cl, 9.40; N, 3.71; Zr, 24.19. Found: C, 41.51; H, 4.28; Cl, 9.40; N, 3.65; Zr, 24.15. Molar conductance (5.7 × $10^{-3}$ M in $CH_2Cl_2$, 25.0 °C): <7.9 × $10^{-3}$ $\Omega^{-1}$ $cm^2$ $mol^{-1}$. $^1H$ NMR (ppm): –3.34 ($CH_3$), –6.17 ($C_5H_5$) in $CDCl_3$; –3.32 ($CH_3$), –6.14 ($C_5H_5$) in $CD_2Cl_2$. IR (Nujol mull) ($cm^{-1}$): $\nu$($C \overset{\cdots}{-} N$) 1525, $\nu$($C \overset{\cdots}{-} S$) 997, $\nu$(Zr—S) 364, $\nu$(Zr—Cl) 340.

**Bis($\eta$-cyclopentadienyl)chloro(*N,N*-diethyldithiocarbamato)zirconium(IV).** This complex was also prepared as described by Jain et al.[15] Recrystallization from dichloromethane–hexane gave clear, colorless crystals of ($\eta$-$C_5H_5$)$_2$ZrCl[$S_2CN(C_2H_5)_2$]; mp 196–201 °C dec (lit.[15] mp 172–175 °C dec). $^1H$ NMR (ppm): –1.25 ($CH_3$, triplet), –3.79 ($CH_2$, quartet), –6.17 ($C_5H_5$) in $CDCl_3$.

**Nuclear Magnetic Resonance Spectra.** Proton chemical shifts were measured at ambient probe temperature (~34 °C) with a Varian EM-390 90-MHz spectrometer. Chemical shifts were measured relative to an internal reference of tetramethylsilane.

Variable-temperature pulsed Fourier-transform $^1H$ NMR spectra of a sealed ~0.1 M solution of ($\eta$-$C_5H_5$)$_2$ZrCl[$S_2CN(CH_3)_2$] in dichloromethane-$d_2$ were recorded in the temperature range –58.6 to +71.1 °C with a Bruker WM-300 300-MHz spectrometer, which was locked on the solvent deuterium resonance. Temperatures, determined with a copper–constantan thermocouple immersed in acetone, are estimated to be accurate to ±0.5 °C.

Rate constants *k* for exchange of dithiocarbamate methyl groups between the two inequivalent environments of ($\eta$-$C_5H_5$)$_2$ZrCl[$S_2CN(CH_3)_2$] were determined by quantitative comparison of experimental spectra with theoretical spectra calculated with use of the Saunders NMR line-shape program.[24] Spectra were compared with respect to the following characteristic line-shape parameters, which were used to determine an average value of *k* at each temperature: (1) line widths at one-fourth ($w_{1/4}$), one-half ($w_{1/2}$), and three-fourths ($w_{3/4}$) maximum amplitude (above the coalescence temperature, $T_c$) and (2) the frequency separation $\delta\nu$ between the two absorption maxima, the ratio *r* of the maximum amplitude to the amplitude at the central minimum, and, where the two resonances are sufficiently well resolved, line widths at three-fourths maximum amplitude (below $T_c$). Line widths and frequency separations in the absence of exchange, $(w_{1/2})_0$ and $\delta\nu_0$, respectively, are both temperature dependent. Values of $(w_{1/2})_0$ appropriate to temperatures in the coalescence region were obtained by extrapolating a linear plot of log $w_{1/2}$ vs. $1/T$ from the fast- and slow-exchange regions into the coalescence region. Appropriate values of ($\delta\nu_0$) in the coalescence region were determined by extrapolating a linear plot of $\delta\nu$ vs. $1/T$ from the slow-exchange region into the coalescence region.

**Crystallography.** Several clear, colorless crystals of ($\eta$-$C_5H_5$)$_2$ZrCl[$S_2CN(C_2H_5)_2$] were sealed in 0.5-mm diameter Lindemann glass capillaries under an atmosphere of dry nitrogen. Weissenberg photographs indicated the crystal system to be monoclinic, and the systematically absent reflections (*h*0*l* for $h + l \neq 2n$ and 0*k*0 for $k \neq 2n$) identified the space group as $P2_1/n$. The lattice constants of $a$ = 17.619 (4) Å, $b$ = 13.892 (3) Å, $c$ = 7.102 (1) Å, and $\beta$ = 93.33 (2)° were determined by least-squares refinement of the diffraction geometry for 15 reflections (2$\theta$ > 16°) centered on a computer-controlled four-circle Syntex P2$_1$ diffractometer using graphite-monochromated Mo K$\bar{\alpha}$ radiation ($\lambda$ 0.71069 Å). The calculated density based on four molecules of ($\eta^5$-$C_5H_5$)$_2$ZrCl[$S_2CN(C_2H_5)_2$] per unit cell is 1.551 g $cm^{-3}$; the observed density, measured by flotation using a solution of carbon tetrachloride and hexane, was 1.549 g $cm^{-3}$.

A rectangular-shaped prism of dimensions 0.67 × 0.19 × 0.07 mm was chosen for collection of intensity data. The data were collected on the Syntex P2$_1$ diffractometer by using the $\theta$–2$\theta$ scan technique with graphite-monochromated Mo K$\bar{\alpha}$ radiation at a takeoff angle of 6.3% and a glancing angle of 2.5°. A variable scan rate ranging from 2°/min for reflections of intensity ≤150 counts/s to 29.3°/min for reflections of intensity ≥1500 counts/s was employed. The range of each scan consisted of a base width of 2.0° at 2$\theta$ = 0° and an increment of $\Delta(2\theta)$ = (0.692 tan $\theta$)° to allow for spectral dispersion; background counts of duration equal to half the total scan time were taken at both limits of the scan. Reflections with intensities greater than 50 000 counts/s were flagged as being too intense to measure and were collected at lower tube current settings. The intensities of three standard reflections, measured at 63-reflection intervals, gave no indication of misalignment or deterioration of the crystal.

A total of 2484 unique reflections having 2$\theta$ ≤ 45.0° (0.62 times the number of data in the limiting Cu K$\bar{\alpha}$ sphere) were scanned. On the basis of the cited dimensions of the crystal and a linear absorption coefficient of 9.95 $cm^{-1}$, the maximum error resulting from neglect of absorption corrections was estimated to be <6.8% in any intensity and <3.4% in any structure amplitude. It was felt that absorption corrections would not significantly improve the reliability of the data. The intensity data were reduced to a set of relative squared amplitudes, $|F_o|^2$, by the application of standard Lorentz and polarization factors. Those 2048 reflections having $|F_o| > 2.0\sigma_F$, where $\sigma_F$ is defined elsewhere,[25] were retained as "observed" for the structure analysis.

**Structure Determination and Refinement.** The structure was solved by application of Patterson and Fourier techniques and was refined by full-matrix least-squares techniques using anisotropic thermal parameters for all 20 non-hydrogen atoms, anomalous dispersion corrections for the Zr, Cl, and S atoms, and $w = 1/\sigma^2$ weighting. The function minimized was $\sum w(|F_o| - |F_c|)^2$. A difference Fourier synthesis upon convergence permitted location of the 20 hydrogen atoms. In subsequent cycles of refinement, the H atoms were assigned fixed positions and isotropic thermal parameters 1.0 Å$^2$ larger than the equivalent isotropic thermal parameter of the attached C atom;

---

[21] Wilson, R. D.; Koetzle, T. F.; Hart, D. W.; Kvick, A.; Tipton, D. L.; Bau, R. *J. Am. Chem. Soc.* **1977**, *99*, 1775.

[22] Green, M. L. H.; McCleverty, J. A.; Pratt, L.; Wilkinson, G. *J. Chem. Soc.* **1961**, 4854.

[23] Klopping, H. L.; van der Kerk, G. J. M. *Recl. Trav. Chim. Pays-Bas* **1951**, *70*, 917.

[24] M. Saunders, Department of Chemistry, Yale University, New Haven, CT.

[25] Radonovich, L. J.; Bloom, A.; Hoard, J. L. *J. Am. Chem. Soc.* **1972**, *94*, 2073.

**Table I.** Final Atomic Fractional Coordinates for $(\eta\text{-}C_5H_5)_2ZrCl[S_2CN(C_2H_5)_2]$ [a]

| atom | $10^4x$ | $10^4y$ | $10^4z$ |
|---|---|---|---|
| Zr | 2699.5 (2) | 5417.0 (3) | 4341.9 (5) |
| Cl | 2075.1 (8) | 4718 (1) | 1304 (2) |
| $S_1$ | 3395.6 (7) | 6179 (1) | 1515 (2) |
| $S_2$ | 3838.0 (8) | 6676 (1) | 5337 (2) |
| N | 4592 (2) | 7301 (3) | 2429 (6) |
| C | 4020 (3) | 6793 (3) | 3013 (6) |
| $C_1$ | 4707 (3) | 7407 (5) | 391 (8) |
| $C_2$ | 5178 (4) | 6625 (6) | −267 (9) |
| $C_3$ | 5157 (3) | 7768 (4) | 3763 (8) |
| $C_4$ | 4955 (3) | 8791 (4) | 4126 (10) |
| $C_{1a}$ | 1646 (4) | 5705 (5) | 6528 (9) |
| $C_{2a}$ | 2120 (3) | 6488 (5) | 6721 (7) |
| $C_{3a}$ | 2059 (3) | 6999 (4) | 5034 (8) |
| $C_{4a}$ | 1569 (3) | 6512 (4) | 3784 (8) |
| $C_{5a}$ | 1317 (3) | 5689 (4) | 4696 (10) |
| $C_{1b}$ | 2790 (6) | 4055 (5) | 6674 (11) |
| $C_{2b}$ | 3455 (7) | 4548 (5) | 6885 (13) |
| $C_{3b}$ | 3834 (3) | 4381 (5) | 5241 (14) |
| $C_{4b}$ | 3386 (4) | 3844 (4) | 4079 (8) |
| $C_{5b}$ | 2732 (4) | 3636 (4) | 4964 (11) |

[a] Numbers in parentheses are estimated standard deviations in the last significant figure.

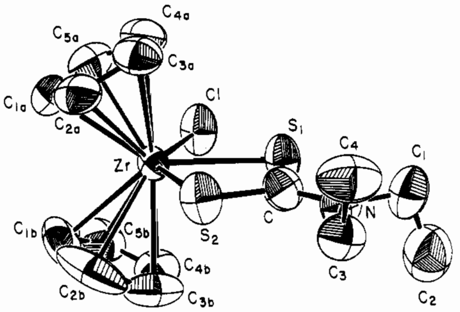

**Figure 1.** Model in perspective of the $(\eta\text{-}C_5H_5)_2ZrCl[S_2CN(C_2H_5)_2]$ molecule. Each atom is represented by an ellipsoid consistent with the thermal parameters in Table II.

the coordinates and anisotropic thermal parameters of the 20 nonhydrogen atoms were allowed to vary as before. In the final cycle of refinement no parameter varied by more than 0.17 (the average was 0.03) of its estimated standard deviation, and the discrepancy indices

$$R_1 = \sum||F_o| - |F_c||/\sum|F_o|$$
$$R_2 = [\sum w(|F_o| - |F_c|)^2/\sum w|F_o|^2]^{1/2}$$

were 0.038 and 0.048, respectively. A final difference Fourier showed no anomalous features; the strongest peak had a density of 0.62 e/Å$^3$.

Scattering factors were taken from Cromer and Mann[26] for $Zr^0$, $Cl^0$, $S^0$, $N^0$, and $C^0$ and from Stewart, Davidson, and Simpson[27] for $H^0$. Anomalous dispersion corrections, real and imaginary, for Zr, Cl, and S were obtained from Cromer.[28] Calculations were performed on PRIME 300 and IBM 370/168 computers using programs listed in a previous paper.[29]

## Results and Discussion

**Solid-State Structure of $(\eta\text{-}C_5H_5)_2ZrCl[S_2CN(C_2H_5)_2]$.** In order to establish the molecular geometry of a representative $(\eta\text{-}C_5H_5)_2ZrCl[S_2CNR_2]$ complex, we have determined the structure of the *N*,*N*-diethyl derivative by X-ray diffraction. Final atomic coordinates and thermal parameters are presented in Tables I and II, respectively. A table of observed and calculated structure factor amplitudes is available.[30] A perspective view of the molecule showing the atom-numbering scheme is displayed in Figure 1; atoms of the two $\eta$-cyclopentadienyl ligands are distinguished by a literal subscript (a or b). Bond distances, nonbonded contacts, and bond angles in the coordination group are given in Table III.

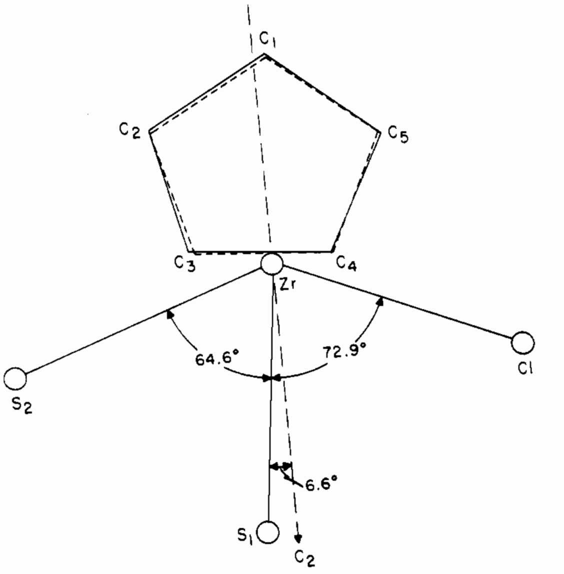

**Figure 2.** Projection of the $ZrClS_2C_{10}$ coordination group onto the quasi mirror plane defined by the atoms Zr, Cl, $S_1$, and $S_2$. Cyclopentadienyl ring a is represented by a solid line; ring b is represented by a dashed line. Also shown is the twofold axis of the $(\eta\text{-}C_5H_5)_2Zr$ fragment, the line that bisects the (centroid $C_5H_5$)–Zr–(centroid $C_5H_5$) angle.

Molecules of $(\eta\text{-}C_5H_5)_2ZrCl[S_2CN(C_2H_5)_2]$ have the bent metallocene geometry **2**, with the Zr atom attached to a Cl atom, a bidentate *N*,*N*-diethyldithiocarbamate ligand, and two symmetrically bound $\eta\text{-}C_5H_5$ ligands. If each $\eta\text{-}C_5H_5$ group is considered to occupy a single coordination site, the Zr atom has coordination number 5. The molecules occupy general positions of the space group $P2_1/n$ and are not required to have any symmetry. However, the $ZrClS_2C_{10}$ coordination group closely approximates $C_s$-*m* symmetry, with the Zr, Cl, $S_1$, and $S_2$ atoms in the quasi mirror plane (atomic displacements ≤0.001 Å; cf. Table VI) and the $\eta\text{-}C_5H_5$ ligands symmetrically disposed on opposite sides of this plane. The $\eta\text{-}C_5H_5$ rings are eclipsed, as is shown in Figure 2, which is a projection of the $ZrClS_2C_{10}$ coordination group onto the quasi mirror plane. Both $\eta\text{-}C_5H_5$ rings are planar, with displacements of the C atoms from the mean planes of the ligands being ≤0.017 Å (cf. Table VI). The angle between the normals to the planes of the two $\eta\text{-}C_5H_5$ ligands (128.9°) agrees closely with the (centroid $C_5H_5$)–Zr–(centroid $C_5H_5$) angle (129.4°), indicating that the Zr–(centroid $C_5H_5$) vectors are nearly orthogonal to the planes of the $\eta\text{-}C_5H_5$ ligands. The dihedral angle between the quasi mirror plane and the plane defined by the Zr atom and the centroids of the $C_5H_5$ rings is 89.5°.

There is considerable crowding in the $ZrClS_2C_{10}$ coordination group, as is evidenced by a number of nonbonded contacts that are appreciably less than the sum of the van der Waals radii.[31] There are four cyclopentadienyl C···Cl contacts ($C_{4a}\cdots Cl$, 3.21 Å; $C_{5a}\cdots Cl$, 3.13 Å; $C_{4b}\cdots Cl$, 3.19 Å; $C_{5b}\cdots Cl$, 3.16 Å), which average 0.33 Å less than the van der Waals contact, and four cyclopentadienyl $C\cdots S_2$ contacts ($C_{2a}\cdots S_2$,

---

(26) Cromer, D. T.; Mann, J. B. *Acta Crystallogr., Sect. A* **1968**, *A24*, 321.

(27) Stewart, R. F.; Davidson, E. R.; Simpson, W. T. *J. Chem. Phys.* **1965**, *42*, 3175.

(28) Cromer, D. T. *Acta Crystallogr., Sect. A* **1965**, *A18*, 17.

(29) Steffen, W. L.; Fay, R. C. *Inorg. Chem.* **1978**, *17*, 2120.

(30) See paragraph at end of paper regarding supplementary material.

(31) We take the van der Waals radii of a cyclopentadienyl carbon atom, chlorine, and sulfur to be 1.7,[32] 1.80,[32] and 1.73 Å,[33] respectively.

(32) Pauling, L. "The Nature of the Chemical Bond", 3rd ed.; Cornell University Press: Ithaca, NY, 1960; p 260.

(33) van der Helm, D.; Lessor, A. E., Jr.; Merritt, L. L., Jr. *Acta Crystallogr.* **1962**, *15*, 1227.

**Table II.** Final Thermal Parameters for $(\eta\text{-}C_5H_5)_2ZrCl[S_2CN(C_2H_5)_2]$[a]

| | anisotropic parameters[b] | | | | | | |
|---|---|---|---|---|---|---|---|
| atom | $B_{11}$ | $B_{22}$ | $B_{33}$ | $B_{12}$ | $B_{13}$ | $B_{23}$ | equiv isotropic $B$,[c] Å$^2$ |
| Zr | 4.55 (2) | 3.31 (2) | 3.04 (2) | 0.12 (2) | 0.12 (1) | −0.22 (1) | 3.57 (1) |
| Cl | 6.97 (7) | 7.92 (8) | 3.91 (6) | −2.73 (6) | 0.01 (5) | −1.27 (5) | 5.61 (5) |
| $S_1$ | 6.21 (7) | 6.36 (7) | 3.65 (5) | −2.04 (6) | 0.09 (5) | −0.21 (5) | 5.05 (4) |
| $S_2$ | 6.78 (7) | 6.24 (7) | 4.29 (6) | −1.78 (6) | −0.39 (5) | −0.81 (5) | 5.45 (4) |
| N | 5.2 (2) | 5.3 (2) | 5.7 (2) | −1.3 (2) | 0.2 (2) | −0.1 (2) | 5.3 (1) |
| C | 5.7 (2) | 4.5 (2) | 4.9 (2) | −0.5 (2) | 0.0 (2) | 0.1 (2) | 5.0 (1) |
| $C_1$ | 5.7 (3) | 7.8 (3) | 6.4 (3) | −1.8 (3) | 1.4 (2) | −0.2 (3) | 6.3 (2) |
| $C_2$ | 8.1 (4) | 14.1 (6) | 6.9 (4) | −1.1 (4) | −0.1 (3) | 1.4 (4) | 9.1 (3) |
| $C_3$ | 5.1 (3) | 5.3 (3) | 7.3 (3) | −0.8 (2) | −0.4 (2) | 0.0 (2) | 5.8 (2) |
| $C_4$ | 6.7 (3) | 5.3 (3) | 11.4 (4) | 0.2 (3) | −1.8 (3) | −0.8 (3) | 7.3 (2) |
| $C_{1a}$ | 7.5 (3) | 7.9 (4) | 6.5 (3) | 2.9 (3) | 3.3 (3) | 1.6 (3) | 6.4 (3) |
| $C_{2a}$ | 7.0 (3) | 7.2 (3) | 4.7 (3) | 2.6 (3) | −0.2 (2) | −1.8 (2) | 5.7 (2) |
| $C_{3a}$ | 6.9 (3) | 4.2 (2) | 6.9 (3) | 1.3 (2) | 0.0 (2) | −0.5 (2) | 5.7 (2) |
| $C_{4a}$ | 6.1 (3) | 6.0 (3) | 6.0 (3) | 2.0 (2) | −0.7 (2) | 0.1 (2) | 5.8 (2) |
| $C_{5a}$ | 4.7 (2) | 6.3 (3) | 8.6 (4) | 0.6 (2) | 1.0 (2) | −0.6 (3) | 6.2 (2) |
| $C_{1b}$ | 15.7 (7) | 6.2 (4) | 7.0 (4) | 5.4 (4) | 4.9 (4) | 3.3 (3) | 6.9 (4) |
| $C_{2b}$ | 18.3 (9) | 5.0 (4) | 7.6 (4) | 4.7 (5) | −6.1 (5) | −1.0 (3) | 7.3 (4) |
| $C_{3b}$ | 5.6 (3) | 5.5 (3) | 12.6 (6) | 1.9 (3) | −1.7 (3) | 0.0 (4) | 6.9 (3) |
| $C_{4b}$ | 8.2 (4) | 4.7 (3) | 6.7 (3) | 1.8 (3) | 1.1 (3) | −1.3 (2) | 6.0 (2) |
| $C_{5b}$ | 8.8 (4) | 3.9 (3) | 9.5 (4) | 0.2 (3) | 0.4 (4) | 1.4 (3) | 6.7 (2) |

[a] Numbers in parentheses are standard deviations in the last significant figure. [b] Anisotropic temperature factors are of the form $\exp[-(\beta_{11}h^2 + \beta_{22}k^2 + \beta_{33}l^2 + 2\beta_{12}hk + 2\beta_{13}hl + 2\beta_{23}kl)]$; the $B_{ij}$ in Å$^2$ are related to the dimensionless $\beta_{ij}$ employed during refinement as $B_{ij} = 4\beta_{ij}/a_i^*a_j^*$. [c] Isotropic thermal parameter calculated from $B = 4[V^2 \det(\beta_{ij})]^{1/3}$.

**Table III.** Bond Distances, Nonbonded Contacts, and Bond Angles Subtended at the Zr(IV) Atom in the Coordination Group of $(\eta\text{-}C_5H_5)_2ZrCl[S_2CN(C_2H_5)_2]$[a]

| | | | |
|---|---|---|---|
| | Lengths, Å | | |
| Zr–Cl | 2.556 (2) | Cl···$C_{4a}$ | 3.208 (6) |
| Zr–$S_1$ | 2.635 (2) | Cl···$C_{5a}$ | 3.128 (7) |
| Zr–$S_2$ | 2.723 (2) | Cl···$C_{4b}$ | 3.188 (6) |
| Zr–$C_{1a}$ | 2.519 (7) | Cl···$C_{5b}$ | 3.163 (7) |
| Zr–$C_{2a}$ | 2.512 (6) | Cl···$S_1$ | 3.084 (2) |
| Zr–$C_{3a}$ | 2.532 (6) | $S_2$···$C_{2a}$ | 3.246 (6) |
| Zr–$C_{4a}$ | 2.520 (5) | $S_2$···$C_{3a}$ | 3.161 (6) |
| Zr–$C_{5a}$ | 2.493 (5) | $S_2$···$C_{2b}$ | 3.239 (8) |
| Zr–$C_{1b}$ | 2.514 (7) | $S_2$···$C_{3b}$ | 3.189 (7) |
| Zr–$C_{2b}$ | 2.693 (9) | $S_1$···$S_2$[b] | 2.865 (2) |
| Zr–$C_{3b}$ | 2.515 (6) | Zr–Cent $Cp_a$[c] | 2.222 (6) |
| Zr–$C_{4b}$ | 2.510 (6) | Zr–Cent $Cp_b$ | 2.216 (7) |
| Zr–$C_{5b}$ | 2.514 (6) | | |
| av Zr–$C_a$ | 2.515 (6,10,22)[d] | | |
| av Zr–$C_b$ | 2.509 (7,7,16)[d] | | |
| | Angles, deg | | |
| $S_1$–Zr–$S_2$ | 64.6 (0) | Cl–Zr–$S_2$ | 137.5 (1) |
| Cl–Zr–$S_1$ | 72.9 (1) | Cent $Cp_a$–Zr–Cent $Cp_b$ | 129.4 (3) |

[a] Numbers in parentheses are estimated standard deviations in the last significant figure. [b] The "bite" of the ligand. [c] Cent Cp refers to the centroid of the cyclopentadienyl ring. [d] The numbers in parentheses following each averaged value are the estimated root-mean-square standard deviation for an individual datum and the mean and maximum deviations from the average value.

**Table IV.** Bond Lengths and Bond Angles in the *N,N*-Diethyldithiocarbamate Ligand[a]

| atoms | length, Å | atoms | angle, deg |
|---|---|---|---|
| $S_1$···$S_2$[b] | 2.865 (2) | $S_1$–C–$S_2$ | 113.8 (3) |
| C–$S_1$ | 1.713 (5) | C–$S_1$–Zr | 92.1 (2) |
| C–$S_2$ | 1.707 (5) | C–$S_2$–Zr | 89.3 (2) |
| C–N | 1.317 (6) | $S_1$–C–N | 121.1 (3) |
| | | $S_2$–C–N | 123.1 (3) |
| $C_1$–N | 1.481 (7) | $C_1$–N–C | 120.8 (4) |
| $C_3$–N | 1.484 (7) | $C_3$–N–C | 122.1 (4) |
| | | $C_1$–N–$C_3$ | 117.1 (4) |
| $C_1$–$C_2$ | 1.459 (10) | N–$C_1$–$C_2$ | 110.6 (5) |
| $C_3$–$C_4$ | 1.492 (8) | N–$C_3$–$C_4$ | 111.6 (4) |

[a] Numbers in parentheses are estimated standard deviations in the last significant figure. [b] The bite of the ligand.

3.25 Å; $C_{3a}$···$S_2$, 3.16 Å; $C_{2b}$···$S_2$, 3.24 Å; $C_{3b}$···$S_2$, 3.19 Å), which average 0.22 Å less than the van der Waals contact. The Cl···$S_1$ distance (3.08 Å) is 0.45 Å less than the sum of the van der Waals radii, and the distance between the closest cyclopentadienyl C atoms ($C_{1a}$···$C_{1b}$, 3.05 Å) is 0.35 Å less than the van der Waals contact between two aromatic rings. The crowding can be attributed to the presence of three relatively large donor atoms in the quasi mirror plane. In this connection, it is interesting to note that the Cl–Zr–$S_2$ angle (137.5°) is 40° larger than the Cl–Zr–Cl angle in $(\eta\text{-}C_5H_5)_2ZrCl_2$.[5]

Because of the crowding in the coordination group, the Zr–Cl and Zr–$S_2$ bond lengths (2.556 (2) and 2.723 (2) Å, respectively) are unusually long. Indeed, to our knowledge, these are the longest terminal Zr–Cl and Zr–S bond lengths yet observed for any structure involving Zr(IV). Typical Zr(IV)–Cl bond lengths are in the range 2.4–2.5 Å;[5,34-40] the Zr–Cl distance in $(\eta\text{-}C_5H_5)ZrCl[S_2CN(C_2H_5)_2]$ is 0.12 Å longer than that in $(\eta\text{-}C_5H_5)_2ZrCl_2$ (2.44 Å).[5] The Zr–$S_2$ distance is 0.09 Å longer than the Zr–$S_1$ distance (2.635 (2) Å). The latter distance may be regarded as a more "normal" Zr–S bond length since sulfur atom $S_1$ makes no repulsive contacts with any of the cyclopentadienyl C atoms. The Zr–$S_1$ distance is intermediate between the Zr–S distances in the four-coordinate oxo-bridged dimeric phenyl mercaptide complex $[(\eta\text{-}C_5H_5)_2Zr(SC_6H_5)]_2O$ (2.542 (2) and 2.554 (2) Å)[41] and the Zr–S distances in the seven-coordinate dithiocarbamate complex $(\eta\text{-}C_5H_5)Zr[S_2CN(CH_3)_2]_3$ (2.655 (1)–2.717 (2) Å)[42] and the eight-coordinate monothiocarbamate complex $Zr[SOCN(C_2H_5)_2]$ (2.669 (1) and 2.689 (1) Å).[29] It is interesting to note (cf. Figure 2) that the Zr–$S_1$ bond does not lie along the $C_2$ axis of the $(\eta\text{-}C_5H_5)_2Zr$ fragment but is rotated by 6.6° in the direction of sulfur atom $S_2$.

---

(34) Kowala, C.; Wunderlich, J. A. *Acta Crystallogr., Sect. B* **1976**, *B32*, 820.
(35) Muir, K. W. *J. Chem. Soc. A* **1971**, 2663.
(36) Saldarriaga-Molina, C. H.; Clearfield, A.; Bernal, I. *J. Organomet. Chem.* **1974**, *80*, 79.
(37) Dusausoy, Y.; Protas, J.; Renaut, P.; Gautheron, B.; Tainturier, G. *J. Organomet. Chem.* **1978**, *157*, 167.
(38) VonDreele, R. B.; Stezowski, J. J.; Fay, R. C. *J. Am. Chem. Soc.* **1971**, *93*, 2887.
(39) Brauer, D. J.; Kruger, C. *Inorg. Chem.* **1975**, *14*, 3053.
(40) Stezowski, J. J.; Eick, H. A. *J. Am. Chem. Soc.* **1969**, *91*, 2890.
(41) Petersen, J. L. *J. Organomet. Chem.* **1979**, *166*, 179.
(42) Bruder, A. H.; Fay, R. C.; Lewis, D. F.; Sayler, A. A. *J. Am. Chem. Soc.* **1976**, *98*, 6932.

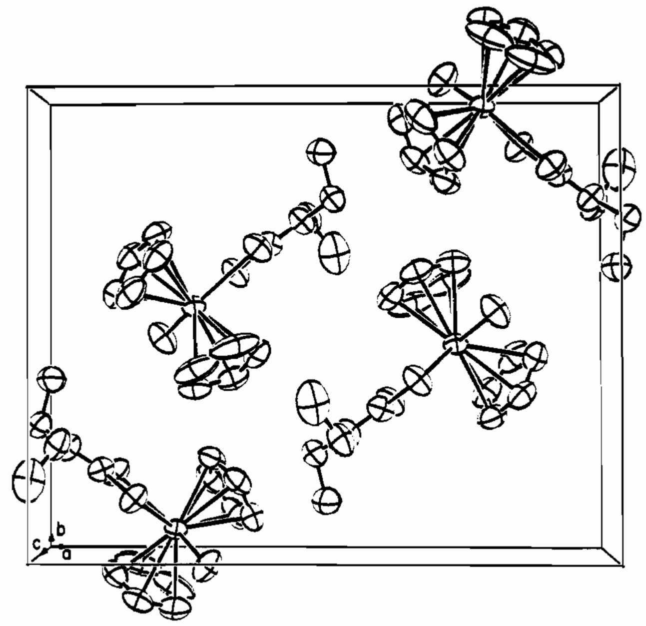

**Figure 3.** Model in perspective to illustrate the packing of ($\eta$-$C_5H_5$)$_2$ZrCl[$S_2CN(C_2H_5)_2$] in the crystal. The contents of one unit cell are viewed normal to the (001) plane.

The ten Zr–C distances are quite uniform (2.493 (5)–2.532 (6) Å; cf. Table III) and are typical of Zr–C distances in other $\eta$-cyclopentadienyl–zirconium structures.[5,10,35,36,41–44] The distances from the Zr atom to the centroids of the $C_5H_5$ rings are 2.222 (6) and 2.216 (7) Å.

**Table V.** Bond Lengths and Bond Angles in the $\eta$-Cyclopentadienyl Ligands[a]

| atoms | length, Å | atoms | angle, deg |
|---|---|---|---|
| $C_{1a}$–$C_{2a}$ | 1.373 (9) | $C_{5a}$–$C_{1a}$–$C_{2a}$ | 108.9 (6) |
| $C_{2a}$–$C_{3a}$ | 1.392 (8) | $C_{1a}$–$C_{2a}$–$C_{3a}$ | 107.6 (5) |
| $C_{3a}$–$C_{4a}$ | 1.380 (8) | $C_{2a}$–$C_{3a}$–$C_{4a}$ | 108.5 (5) |
| $C_{4a}$–$C_{5a}$ | 1.398 (8) | $C_{3a}$–$C_{4a}$–$C_{5a}$ | 107.9 (5) |
| $C_{5a}$–$C_{1a}$ | 1.394 (9) | $C_{4a}$–$C_{5a}$–$C_{1a}$ | 107.0 (5) |
| av C–C[b] | 1.387 (8,9,14) | av C–C–C[b] | 108.0 (5,6,10) |
| $C_{1b}$–$C_{2b}$ | 1.358 (15) | $C_{5b}$–$C_{1b}$–$C_{2b}$ | 109.7 (8) |
| $C_{2b}$–$C_{3b}$ | 1.397 (14) | $C_{1b}$–$C_{2b}$–$C_{3b}$ | 105.9 (7) |
| $C_{3b}$–$C_{4b}$ | 1.336 (10) | $C_{2b}$–$C_{3b}$–$C_{4b}$ | 108.4 (7) |
| $C_{4b}$–$C_{5b}$ | 1.375 (10) | $C_{3b}$–$C_{4b}$–$C_{5b}$ | 108.4 (6) |
| $C_{5b}$–$C_{1b}$ | 1.345 (11) | $C_{4b}$–$C_{5b}$–$C_{1b}$ | 107.5 (7) |
| av C–C[b] | 1.362 (12,19,35) | av C–C–C[b] | 108.0 (7,10,21) |

[a] Numbers in parentheses are estimated standard deviations in the last significant figure. [b] The numbers in parentheses following each averaged value are the root-mean-square estimated standard deviation for an individual datum and the mean and maximum deviations from the average value.

**Table VI**

Least-Squares Mean Planes of the Form $AX + BY + CZ = D$[a]

| plane no. | atoms | $A$ | $B$ | $C$ | $D$ |
|---|---|---|---|---|---|
| 1 | Zr, Cl, $S_1$, $S_2$ | −0.6563 | 0.7534 | −0.0417 | 2.5362 |
| 2 | $S_1$, $S_2$, C, N, $C_1$, $C_3$ | −0.5749 | 0.8168 | −0.0491 | 3.5949 |
| 3 | $C_{1a}$, $C_{2a}$, $C_{3a}$, $C_{4a}$, $C_{5a}$ | −0.7863 | 0.5280 | 0.3208 | 3.5823 |
| 4 | $C_{1b}$, $C_{2b}$, $C_{3b}$, $C_{4b}$, $C_{5b}$ | −0.4088 | 0.8214 | −0.3977 | 0.8608 |

Atoms and Their Displacements from Planes, Å

| | |
|---|---|
| plane 1 | Zr, 0.001; Cl, −0.001; $S_1$, 0.000; $S_2$, −0.001; C, −0.083; N, −0.210[b] |
| plane 2 | $S_1$, −0.041; $S_2$, 0.033; C, 0.007; N, 0.011; $C_1$, 0.037; $C_3$, −0.047; Zr, −0.231 |
| plane 3 | $C_{1a}$, 0.017; $C_{2a}$, −0.015; $C_{3a}$, 0.007; $C_{4a}$, 0.004; $C_{5a}$, −0.013 |
| plane 4 | $C_{1b}$, −0.012; $C_{2b}$, 0.015; $C_{3b}$, −0.013; $C_{4b}$, 0.005; $C_{5b}$, 0.005 |

[a] $X$, $Y$, and $Z$ are orthogonal coordinates measured in Å along $a$, $b$, and $c^*$, respectively, of the crystallographic coordinate system. [b] A displacement in the negative direction is toward $C_5H_5$ ring b.

Bond lengths and angles within the dithiocarbamate ligand (Table IV) are in agreement with values found in other dithiocarbamate structures.[42,45–55] The bite of the ligand (2.865 (2) Å) agrees well with values reported for ($\eta$-$C_5H_5$)Zr[$S_2CN(CH_3)_2$]$_3$.[42] Delocalized $\pi$ bonding in the $S_1S_2CN$ portion of the ligand is indicated by the C–N (1.317 Å) and C–S (average 1.710 Å) distances, which are intermediate between single-bond and double-bond distances (C—N, 1.47 Å; C=N, 1.27 Å; C—S, 1.81 Å; C=S, 1.61 Å).[56] Accordingly, the $S_1S_2CNC_1C_3$ portion of the dithiocarbamate ligand (cf. Figure 1) is nearly planar, the mean and maximum displacements of these atoms from the mean plane being 0.029 and 0.047 Å, respectively (cf. Table VI). Such departures from planarity as are observed correspond to a slight twisting of the ligand about the C–N bond; the dihedral angle between the $S_1S_2CN$ and $CNC_1C_3$ mean planes is 3.4°. The terminal methyl groups are located on opposite sides of the plane defined by the $S_1S_2CNC_1C_3$ portion of the ligand. The Zr atom is displaced from this plane by 0.231 Å, which implies a small folding of the chelate ring about the S···S vector; the dihedral angle between the $S_1S_2CNC_1C_3$ plane and the $ZrS_1S_2$ plane is 5.9°. The chelate ring is folded so as to bend the uncoordinated part of the ligand in the direction of $C_5H_5$ group b. Both the ring folding and the ligand twisting can be rationalized in terms of a short intermolecular contact ($C_4$···$C_4$, 3.58 Å) between methyl groups of adjacent molecules. The only other intermolecular contact that is appreciably less than the sum of the van der Waals radii involves a cyclopentadienyl and a methylene carbon atom ($C_{3b}$···$C_3$, 3.53 Å). A packing diagram is presented in Figure 3.

Bond lengths and angles within the cyclopentadienyl ligands are listed in Table V. Carbon–carbon distances are quite uniform in ligand a (1.373–1.398 Å) but somewhat more varied in ligand b (1.336–1.397 Å). However, this variation is not considered significant in view of the larger esd's on the C–C distances in ring b (Table V) and the highly anisotropic thermal parameters observed for the carbon atoms in ring b (Table II). The averaged C–C bond length for both rings (1.375 Å) is in good agreement with corresponding values obtained for other $\eta$-cyclopentadienyl–zirconium structures.[5,10,35,36,41–44]

**Kinetics of Methyl Group Exchange in ($\eta$-$C_5H_5$)$_2$ZrCl[$S_2CN(CH_3)_2$].** $^1$H NMR spectra of ($\eta$-$C_5H_5$)$_2$ZrCl[$S_2CN$-

---

(43) Sim, G. A.; Bush, M. A. *J. Chem. Soc. A* **1971**, 2225.

(44) Anderson, S. J.; Brown, D. S.; Finney, K. J. *J. Chem. Soc., Dalton Trans.* **1979**, 152.

(45) (a) Coucouvanis, D. *Prog. Inorg. Chem.* **1970**, *11*, 233. (b) Eisenberg, R. *Ibid.* **1970**, *12*, 295. (c) Coucouvanis, D. *Ibid.* **1979**, *26*, 301.

(46) Lewis, D. F.; Fay, R. C. *J. Am. Chem. Soc.* **1974**, *96*, 3843.

(47) Lewis, D. F.; Fay, R. C. *Inorg. Chem.* **1976**, *15*, 2219.

(48) Dewan, J. C.; Kepert, D. L.; Raston, C. L.; Taylor, D.; White, A. H.; Maslen, E. N. *J. Chem. Soc., Dalton Trans.* **1973**, 2082.

(49) (a) Brennan, T. F.; Bernal, I. *Chem. Commun.* **1970**, 138. (b) Brennan, T. F.; Bernal, I. *Inorg. Chim. Acta* **1973**, *7*, 283.

(50) (a) Colapietro, M.; Vaciago, A.; Bradley, D. C.; Hursthouse, M. B.; Rendall, I. F. *J. Chem. Soc., Dalton Trans.* **1972**, 1052. (b) Colapietro, M.; Domenicano, A.; Vaciago, A. *Chem. Commun.* **1968**, 572.

(51) (a) Healy, P. C.; White, A. H. *J. Chem. Soc., Dalton Trans.* **1972**, 1163. (b) Healy, P. C.; White, A. H.; Hoskins, B. F. *Ibid.* **1972**, 1369. (c) Newman, P. W. G.; White, A. H. *Ibid.* **1972**, 1460. (d) Healy, P. C.; White, A. H. *Ibid.* **1972**, 1883. (e) Healy, P. C.; White, A. H. *Ibid.* **1973**, 284. (f) Raston, C. L.; White, A. H. *Ibid.* **1974**, 1790.

(52) Ciampolini, M.; Mengozzi, C.; Orioli, P. *J. Chem. Soc., Dalton Trans.* **1975**, 2051.

(53) (a) Pignolet, L. H. *Inorg. Chem.* **1974**, *13*, 2051. (b) Abrahamson, H.; Heiman, J. R.; Pignolet, L. H. *Ibid.* **1975**, *14*, 2070.

(54) (a) Ricard, L.; Martin, C.; Wiest, R.; Weiss, R. *Inorg. Chem.* **1975**, *14*, 2300. (b) Kopwillem, A. *Acta Chem. Scand.* **1972**, *26*, 2941.

(55) Harreld, C. S.; Schlemper, E. O. *Acta Crystallogr., Sect. B* **1964**, *B27*, 1964.

(56) Reference 32, pp 224–229.

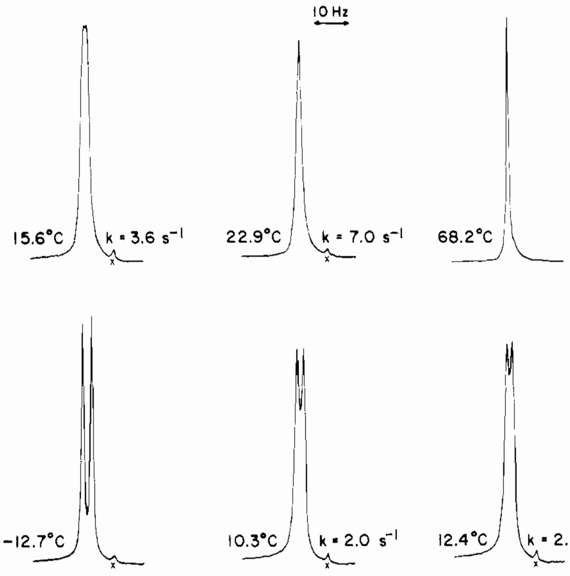

**Figure 4.** Methyl proton resonances of $(\eta\text{-}C_5H_5)_2ZrCl[S_2CN(CH_3)_2]$, ~0.1 M in $CD_2Cl_2$, at 300 MHz. The peak marked with an × is due to an unidentified impurity.

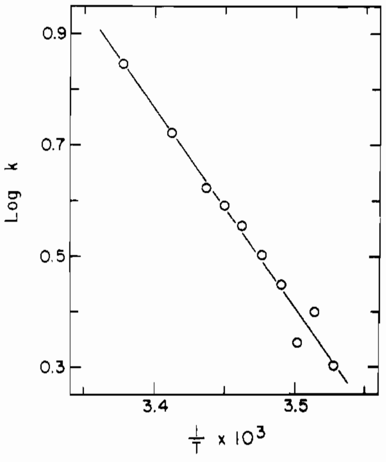

**Figure 5.** Arrhenius plot for methyl group exchange in $(\eta\text{-}C_5H_5)_2ZrCl[S_2CN(CH_3)_2]$.

$(CH_3)_2]$ in $CD_2Cl_2$ solution have been recorded at 300 MHz in the temperature range −58.6 to +71.1 °C. In the slow-exchange limit, this complex exhibits two closely spaced methyl proton resonances of equal intensity (cf. Figure 4), consistent with the bent metallocene structure found for solid $(\eta\text{-}C_5H_5)_2ZrCl[S_2CN(C_2H_5)_2]$ (Figure 1). The two methyl resonances coalesce at ~16 °C to give one line, which sharpens with increasing temperature. A single, sharp cyclopentadienyl proton resonance is observed at all temperatures.

Rates of exchange of methyl groups between the two inequivalent sites of the bent metallocene structure were determined by total line-shape analysis as described in the Experimental Section. Rate constants and characteristic line-shape parameters are listed in Table VII along with Arrhenius and Eyring activation parameters, which were obtained from the least-squares straight lines of a log $k$ vs. $1/T$ plot (Figure 5) and a log $(k/T)$ vs. $1/T$ plot. The barrier to exchange is ~16 kcal/mol, and the rate constant at 25 °C is 8.6 $s^{-1}$. Estimates of error on the activation parameters are relatively large because the small frequency separation between the two methyl resonances (2.05–2.26 Hz, ~0.007 ppm, in the coalescence region) severely restricts the temperature range over which reliable rate constants can be determined. In 300-MHz $^1H$ NMR spectra of $(\eta\text{-}C_5H_5)_2ZrCl[S_2CN(CH_3)_2]$ in $CHClF_2$ solution, the methyl resonances remain unresolved at temperatures down to −150 °C! The near-degeneracy in the chemical shifts is surprising in view of the approximately 10 times larger shifts (~0.07 ppm) for the methyl resonances of $(\eta\text{-}C_5H_5)Zr[S_2CN(CH_3)_2]_3$.[42]

Table VII

Kinetic Data for Exchange of Methyl Groups in $(\eta\text{-}C_5H_5)_2ZrCl[S_2CN(CH_3)_2]$[a]

| temp, °C | line widths, Hz | | | $\delta\nu$,[c] Hz | $r$[d] | $k$, $s^{-1}$ |
|---|---|---|---|---|---|---|
| | $w_{1/4}$ | $w_{1/2}$[b] | $w_{3/4}$ | | | |
| 22.9 | 3.09 | 1.84 | 1.06 | | | 7.0 |
| 19.9 | 3.60 | 2.23 | 1.39 | | | 5.3 |
| 17.8 | 3.90 | 2.59 | 1.84 | | | 4.2 |
| 16.7 | 3.96 | 2.79 | 2.09 | | | 3.9 |
| 15.6 | 4.07 | 2.93 | 2.26 | 0.75 | 1.02 | 3.6 |
| 14.5 | | | | 1.10 | 1.05 | 3.2 |
| 13.4 | | | | 1.42 | 1.12 | 2.8 |
| 12.4 | | | | 1.89 | 1.18 | 2.2 |
| 11.4 | | | | 1.56 | 1.29 | 2.5 |
| 10.3 | | | 0.95 | 1.86 | 1.43 | 2.0 |

Activation Parameters[e]

| | | | |
|---|---|---|---|
| $E_a$, kcal/mol | 16.5 ± 2.0 | $T_c$,[f] °C | 16 |
| log $A$ | 13.0 ± 1.5 | $\Delta G^{\ddagger}(T_c)$, kcal/mol | 16.17 ± 0.08 |
| $\Delta H^{\ddagger}$, kcal/mol | 15.9 ± 2.0 | $\Delta G^{\ddagger}$(25 °C), kcal/mol | 16.18 ± 0.08 |
| $\Delta S^{\ddagger}$, eu | −1.0 ± 6.8 | $k$(25 °C), $s^{-1}$ | 8.6 |

[a] ~$10^{-1}$ M in $CD_2Cl_2$. [b] The line width at half-maximum amplitude in the absence of exchange, $(w_{1/2})_0$, varies from 0.80 Hz at 22.9 °C to 0.83 Hz at 10.3 °C. [c] The frequency separation in the absence of exchange, $(\delta\nu)_0$, varies from 2.05 Hz at 22.9 °C to 2.26 Hz at 10.3 °C. [d] Ratio of the maximum amplitude to the amplitude at the central minimum. [e] The uncertainties in the activation parameters are random errors estimated at the 95% confidence level. [f] Coalescence temperature.

Possible mechanisms for methyl group exchange in $(\eta\text{-}C_5H_5)_2ZrCl[S_2CN(CH_3)_2]$ are outlined in Figure 6. These include (a) dissociation of the dithiocarbamate ligand, (b) dissociation of $Cl^-$ to give a symmetrical four-coordinate intermediate, (c) a digonal twist of the entire planar dithiocarbamate ligand about its twofold axis, (d) chloride migration involving a trigonal-bipyramidal transition state, (e) Zr–S bond rupture to give a four-coordinate intermediate, followed by rotation of the dangling ligand about the Zr—S and/or C—S bonds and subsequent reattachment of the uncoordinated S atom at the other sulfur coordination site, (f) Zr—S bond rupture followed by rotation about the C=N partial double bond and subsequent reattachment of the uncoordinated S atom, and (g) rotation about the C=N bond without Zr–S bond rupture. One can, of course, envision a continuum of mechanisms intermediate between (f) and (g) that involve rotation about the C=N bond accompanied by more or less Zr—S bond stretching.

Dissociative mechanisms a and b are ruled out by the following $^1H$ NMR results obtained at 34 °C and 90 MHz: (1) the spectrum of a $CD_2Cl_2$–$CD_3CN$ (1:1 v/v) solution containing both $(\eta\text{-}C_5H_5)_2ZrCl[S_2CN(CH_3)_2]$ (0.035 M) and $Na[S_2CN(CH_3)_2]$ (0.093 M) showed separate methyl resonances for each compound; (2) the spectrum of a $CD_2Cl_2$ solution of $(\eta\text{-}C_5H_5)_2ZrCl[S_2SN(CH_3)_2]$ and $(\eta\text{-}C_5H_5)_2ZrBr[S_2CN(CH_3)_2]$ (both ~0.1 M) showed separate methyl resonances for each complex. In each case, the line width of the methyl resonance of $(\eta\text{-}C_5H_5)_2ZrCl[S_2CN(CH_3)_2]$ (0.62 Hz) was essentially the same as that in the absence of added $Na[S_2CN(CH_3)_2]$ or $(\eta\text{-}C_5H_5)_2ZrBr[S_2CN(CH_3)_2]$. These experiments show that dithiocarbamate ligand exchange and halide ligand exchange are slow on the NMR time scale at a temperature 18 °C above the coalescence temperature for methyl group exchange. Therefore, the mechanism of methyl group exchange cannot involve complete dissociation of dithiocarbamate or chloride ions. The absence of any appreciable equilibrium concentration of ions in di-

**Table VIII.** Kinetic Data for Exchange of Methyl Groups in *N,N*-Dimethyldithiocarbamate Compounds[a]

| compd | solvent | $k$(25 °C), s$^{-1}$ | $\Delta G^{\ddagger}$(25 °C), kcal/mol | $\Delta H^{\ddagger}$, kcal/mol | $\Delta S^{\ddagger}$, eu | ref |
|---|---|---|---|---|---|---|
| $CH_3SC(S)N(CH_3)_2$ | *n*-hexane | 107 | 14.7 ± 0.2 | 9.7 ± 0.6 | −17 ± 2 | 58[b] |
| | *n*-hexane | | 14.7 | 12.5 | −7 | 59 |
| $[SC(S)N(CH_3)_2]_2$ | $CD_2Cl_2$ | 16 | 15.8 | 17.8 | 7 ± 4 | 60 |
| $(\eta\text{-}C_5H_5)_2ZrCl[S_2CN(CH_3)_2]$ | $CD_2Cl_2$ | 8.6 | 16.2 ± 0.1 | 15.9 ± 2.0 | −1 ± 7 | this work |

[a] Uncertainties in the activation parameters for $CH_3SC(S)N(CH_3)_2$ and $(\eta\text{-}C_5H_5)_2ZrCl[S_2CN(CH_3)_2]$ are random errors estimated at the 95% confidence level. [b] The values listed were calculated from kinetic data in ref 58.

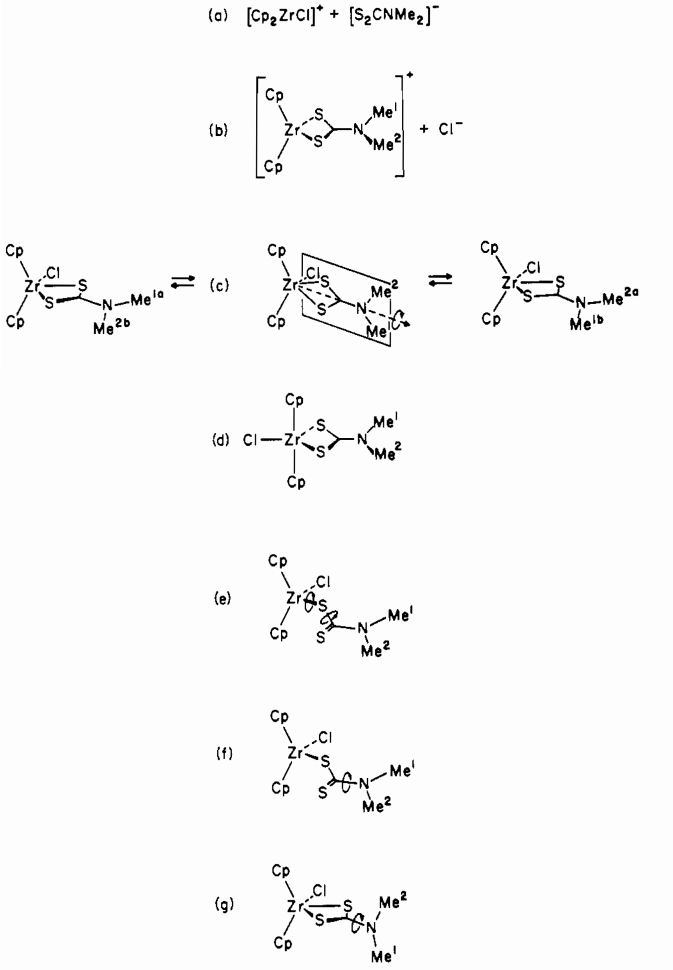

**Figure 6.** Possible mechanisms for methyl group exchange in $(\eta\text{-}C_5H_5)_2ZrCl[S_2CN(CH_3)_2]$. All of these mechanisms exchange methyl groups 1 and 2 between inequivalent sites a and b. Microscopic reversibility requires that the intermediate in mechanism e must form by rupture of either Zr–S bond.

chloromethane solutions is indicated by a molar conductance of <7.9 × $10^{-3}$ $\Omega^{-1}$ cm$^2$ mol$^{-1}$ for a 5.7 × $10^{-3}$ M solution.

The digonal twist and chloride migration mechanisms, (c) and (d) in Figure 6, are unlikely because the transition states are even more crowded than the already congested bent metallocene structure. For example, if the observed Zr—Cl, Zr—S, and Zr—C bond lengths are maintained in the trigonal-bipyramidal transition state of mechanism d, the C⋯Cl and C⋯S nonbonded contacts would be 0.3–0.4 Å shorter than in the observed structure and 0.5–0.7 Å less than the sum of the van der Waals radii. Extended Hückel calculations on the model compound $(\eta\text{-}C_5H_5)_2ZrCl(S_2CH)$ (vide infra) give calculated barriers for mechanisms c and d of 70 and 95 kcal/mol, respectively. These barriers, which are more than 4 times the observed barrier, are due to both steric and electronic effects.

Mechanisms e and f are attractive because Zr–S bond rupture relieves steric crowding in the coordination group and because the unusually long bond to the S atom in the lateral coordination site ($Zr\text{–}S_2$ in Figure 1) should be especially susceptible to bond rupture. Indeed we have considered the possibility that $(\eta\text{-}C_5H_5)_2ZrCl[S_2CN(CH_3)_2]$ might exist in solution as a four-coordinate complex that contains a monodentate dithiocarbamate ligand. This, however, is unlikely since solid-state and dichloromethane-solution infrared spectra of $(\eta\text{-}C_5H_5)_2ZrCl[S_2CN(CH_3)_2]$ are essentially identical; for solid and solution, one observes a single $\nu$(C$\overset{..}{-}$S) band, characteristic of bidentate dithiocarbamate.[57] Moreover, solid-state infrared spectra of $(\eta\text{-}C_5H_5)_2ZrCl[S_2CN(CH_3)_2]$ and $(\eta\text{-}C_5H_5)_2ZrCl[S_2CN(C_2H_5)_2]$ are similar,[15] and the solid-state structure of the *N,N*-diethyl derivative has been shown, in the present work, to contain bidentate dithiocarbamate. $^1$H NMR spectroscopy of $CD_2Cl_2$ solutions of $(\eta\text{-}C_5H_5)_2ZrCl[S_2CN(CH_3)_2]$ at 300 MHz detects only one isomer at all temperatures investigated. Taken together, the IR and NMR evidence indicate that the five-coordinate, chelated bent metallocene is the major species in dichloromethane solution and that the four-coordinate, ring-opened isomer is present in no more than small, undetectable concentrations. The ring-opened isomer, however, could be present as a low-concentration reaction intermediate.

Strong evidence for a mechanism involving C$\overset{..}{-}$N bond rotation, (f) or (g) in Figure 6, comes from a comparison of kinetic data for $(\eta\text{-}C_5H_5)_2ZrCl[S_2CN(CH_3)_2]$ with kinetic data for methyl *N,N*-dimethyldithiocarbamate[58,59] and *N,N,N′,N′*-tetramethylthiuram disulfide[60] (cf. Table VIII). The methyl ester and thiuram disulfide exhibit a similar exchange of *N*-methyl groups, with values of $k$ and $\Delta G^*$ at 25 °C that differ from those for $(\eta\text{-}C_5H_5)_2ZrCl[S_2CN(CH_3)_2]$ by factors of $\lesssim$10 and $\leq$1.5 kcal/mol, respectively. Values of $\Delta H^*$ and $\Delta S^*$ (Table VIII) vary more widely, but it is the rate constant and $\Delta G^*$ in the coalescence region that are the most accurately determined kinetic parameters. In the case of the organic derivatives, the kinetic process must involve C$\overset{..}{-}$N bond rotation. A similar process is expected in the zirconium complex.

The slightly higher barrier for methyl group exchange in $(\eta\text{-}C_5H_5)_2ZrCl[S_2CN(CH_3)_2]$ relative to the barriers in the organic derivatives can be rationalized in terms of mechanism f or g. When the dithiocarbamate ligand is attached to an electropositive metal like Zr(IV), resonance structure **4c** will

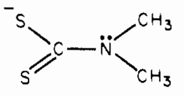

4a

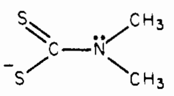

4b

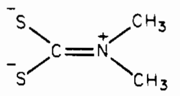

4c

be relatively more important, and resonance structures **4a** and **4b** relatively less important, than in the organic derivatives. Thus, a higher barrier to C$\overset{..}{-}$N bond rotation is expected in the zirconium complex, especially if the dithiocarbamate ligand remains bidentate as in mechanism g. Experimental evidence

---

(57) Bonati, F.; Ugo, R. *J. Organomet. Chem.* **1967**, *10*, 257.

(58) Holloway, C. E.; Gitlitz, M. H. *Can. J. Chem.* **1967**, *45*, 2659.

(59) Lemire, A. E.; Thompson, J. C. *Can. J. Chem.* **1970**, *48*, 824.

(60) Edgar, B. L.; Duffy, D. J.; Palazzotto, M. C.; Pignolet, L. H. *J. Am. Chem. Soc.* **1973**, *95*, 1125.

for a higher barrier to $\mathrm{C}\overset{\cdots}{-}\mathrm{N}$ rotation in bidentate dithiocarbamate than in monodentate dithiocarbamate is provided by an NMR study of $Rh[P(C_6H_5)_3][S_2CN(CH_3)_2]_3$.[61] This complex exhibits five methyl proton resonances of relative intensity 2:1:1:1:1 at 27 °C, consistent with an octahedral structure containing one monodentate dithiocarbamate ligand cis to the $P(C_6H_5)_3$ group and two bidentate dithiocarbamate ligands. The resonance of relative intensity 2 is reasonably assigned to the methyl groups of the monodentate dithiocarbamate, which are exchanging rapidly due to rapid $\mathrm{C}\overset{\cdots}{-}\mathrm{N}$ bond rotation in the monodentate ligand. Rotation about the $\mathrm{C}\overset{\cdots}{-}\mathrm{N}$ bond in the bidentate ligands is slower; all five methyl resonances do not coalesce until 72 °C.

If methyl group exchange in $(\eta\text{-}C_5H_5)_2ZrCl[S_2CN(CH_3)_2]$ occurs by mechanism f, the barrier to exchange will be increased beyond that needed for $\mathrm{C}\overset{\cdots}{-}\mathrm{N}$ bond rotation in the monodentate ligand by the free energy difference between the four-coordinate, ring-opened isomer and the five-coordinate, chelated isomer. The latter free energy difference must be at least 1.5 kcal/mol, or else the ring-opened isomer would be observed by NMR. However, extended Hückel calculations (vide infra) indicate no significant energy difference between the ring-opened and chelated isomers. Thus the increase in the barrier height due to Zr–S bond rupture may be quite modest. The ease of metal–ligand bond rupture in five-coordinate zirconocene complexes is illustrated by a recent study of the analogous ylide complex $(\eta\text{-}C_5H_5)_2ZrCl[(CH_2)_2P(CH_3)_2]$.[62] This compound undergoes exchange of the inequivalent methylene groups ($\Delta G^{\ddagger}(50\ °C) \approx 15.5$ kcal/mol) by a proposed mechanism that involves Zr–C bond rupture and formation of the symmetrical four-coordinate intermediate $(\eta\text{-}C_5H_5)_2ZrCl[(CH_2)P(CH_2)(CH_3)_2]$. Also relevant here is the solid-state structure of $(\eta\text{-}C_5H_5)_2ZrCl[CH_2P(C_6H_5)_2]$, which exists as the four-coordinate ring-opened isomer; the phosphinomethyl C atom is attached to the Zr atom, but the Zr and P atoms avoid each other.[63]

The following conclusions may be drawn in summary of our discussion relating to the mechanisms outlined in Figure 6. (1) Dissociative mechanisms a and b can be ruled out on experimental grounds. (2) Polytopal rearrangement mechanisms c and d are unlikely for steric reasons and can be discarded on the basis of extended Hückel calculations. (3) Bond-rupture mechanism e cannot be ruled out since metal–ligand bond rupture should be a facile process in five-coordinate zirconocenes; however, this mechanism is not needed to account for methyl group exchange in $(\eta\text{-}C_5H_5)_2ZrCl[S_2CN(CH_3)_2]$ because comparison of kinetic data for the zirconium complex and related organic dithiocarbamates indicates that the observed rate process almost certainly involves rotation about the $\mathrm{C}\overset{\cdots}{-}\mathrm{N}$ bond. (4) Extended Hückel calculations confirm the ease of Zr—S bond rupture in $(\eta\text{-}C_5H_5)_2ZrCl(S_2CNR_2)$ systems, thus favoring mechanism f over mechanism g. However, the presently available experimental data do not distinguish between these two possibilities. In an effort to clarify this point, we plan to investigate the structure and dynamics of other $(\eta\text{-}C_5H_5)_2ZrX[S_2CN(CH_3)_2]$ complexes, where the size and electronic properties of the monodentate ligand X will be varied.

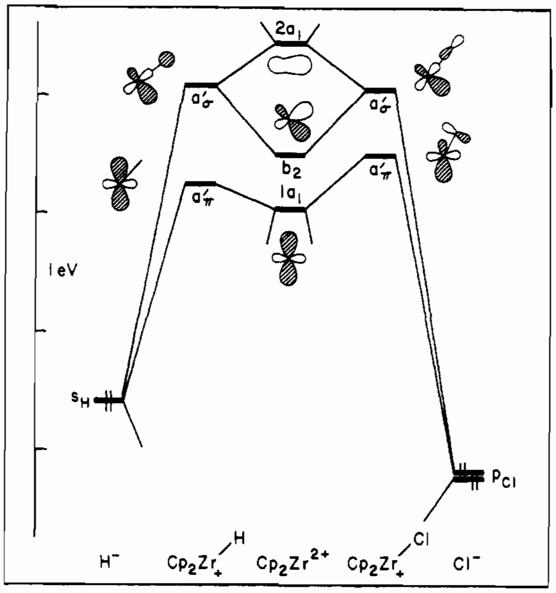

**Figure 7.** Interaction diagram for $(\eta\text{-}C_5H_5)_2ZrH^+$ (left) and $(\eta\text{-}C_5H_5)_2ZrCl^+$ (right).

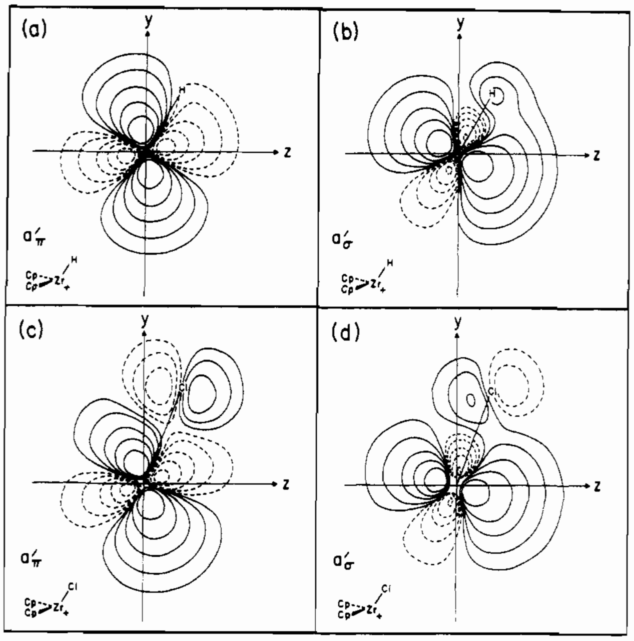

**Figure 8.** Contour plots of the $a'_\pi$ and $a'_\sigma$ orbitals for $(\eta\text{-}C_5H_5)_2ZrH^+$ (a, b) and $(\eta\text{-}C_5H_5)_2ZrCl^+$ (c, d). The values of the wave function at the contours are ±0.20, ±0.10, ±0.055, ±0.025, and ±0.010.

**Theoretical Analysis of $(\eta\text{-}C_5H_5)_2ZrCl(S_2CNR_2)$ Complexes. A. Equilibrium Geometry.** The electronic structure of $(\eta\text{-}C_5H_5)_2ML_n$ complexes has been thoroughly analyzed in terms of interaction of the bent $(\eta\text{-}C_5H_5)_2M$ moiety with the *n* ligands L.[2] In $C_{2v}$ symmetry, the $(\eta\text{-}C_5H_5)_2M$ fragment has three low-lying orbitals $1a_1$, $b_2$, and $2a_1$ (Figure 7) and two high-lying orbitals $b_1$ and $a_2$. The $b_1$ and $a_2$ orbitals are destabilized by strong interaction with the $\pi$ orbitals of the $\eta\text{-}C_5H_5$ rings; only the three low-lying orbitals are capable of bonding with additional ligands L. Since these orbitals have their extension in the mirror plane that bisects the (centroid $C_5H_5$)–Zr–(centroid $C_5H_5$) angle, the ligands L lie in this mirror plane. For a $d^0$ metal, a maximum of three ligands can be accommodated.

The geometry of an $(\eta\text{-}C_5H_5)_2ZrCl(S_2CNR_2)$ complex is conveniently investigated by considering the interaction of $(\eta\text{-}C_5H_5)_2ZrCl^+$ and $S_2CNR_2^-$ fragments. The valence orbitals of an $(\eta\text{-}C_5H_5)_2ZrL$ fragment are easily derived from the valence orbitals of $(\eta\text{-}C_5H_5)_2Zr$ and L fragments (cf. Figure 7). If the ligand L is mainly a $\sigma$ donor, for example $H^-$, the $1a_1$ orbital of $(\eta\text{-}C_5H_5)_2Zr$ is only slightly perturbed by L since L is situated very near the nodal plane of $1a_1$ (cf. Figure 8a). Because of slight mixing with the $b_2$ and $2a_1$ orbitals, the $1a_1$ orbital increases its extension toward the vacant site of (η-

---

(61) Davis, R.; Hill, M. N. S.; Holloway, C. E.; Johnson, B. F. G.; Al-Obaidi, K. H. *J. Chem. Soc. A* **1971**, 994.

(62) Gell, K. I.; Schwartz, J. *Inorg. Chem.* **1980**, *19*, 3207.

(63) Schore, N. E.; Hope, H. *J. Am. Chem. Soc.* **1980**, *102*, 4251.

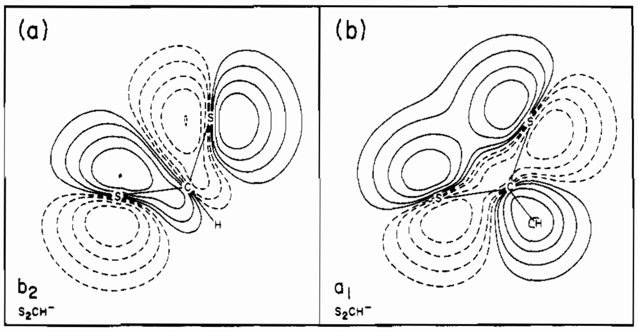

**Figure 9.** Contour plots of the $b_2$ and $a_1$ orbitals of $S_2CH^-$. The contour values are the same as in Figure 8.

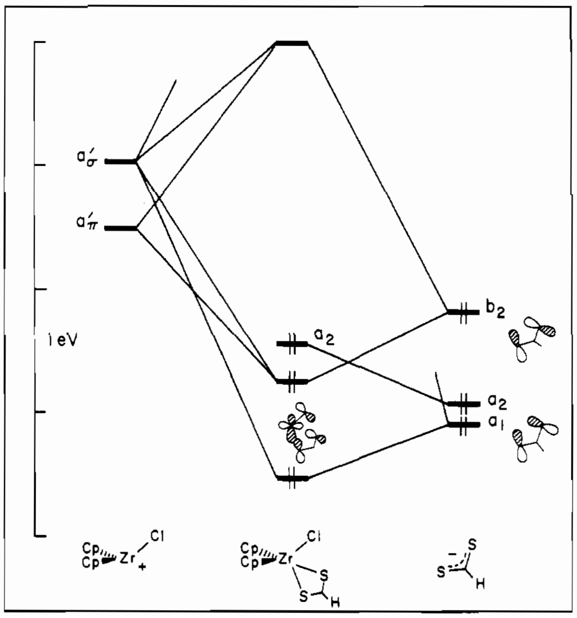

**Figure 10.** Interaction diagram for the chelated isomer of ($\eta$-$C_5H_5)_2ZrCl(S_2CH)$.

$C_5H_5)_2ZrL$, i.e. the site of the second ligand in ($\eta$-$C_5H_5)_2ZrL_2$. Although the ($\eta$-$C_5H_5)_2ZrL$ fragment has no symmetry other than the bisecting mirror plane, it is evident from Figure 8a that the orbital of $1a_1$ parentage has definite $\pi$-type character with respect to the vacant site. This orbital will be called $a'_\pi$; it is the LUMO of the ($\eta$-$C_5H_5)_2ZrL$ fragment (cf. Figure 7). The second low-lying orbital results from strong mixing of the $b_2$ and $2a_1$ orbitals, both of which overlap well with the $\sigma$ orbital of the ligand L. As Figure 8b shows, this orbital has $\sigma$ character with respect to the vacant site; it will be referred to as $a'_\sigma$. The hybridization of $a'_\sigma$ toward the vacant site is the usual consequence of decreasing the antibonding Zr–L interaction by mixing in metal p orbitals.

If the ligand L is a $\pi$ donor, for example $Cl^-$, the $a'_\pi$ orbital is raised in energy (cf. Figure 7) because it has the proper local symmetry to interact with the ligand $\pi$ orbital (cf. Figure 8c). On the other hand, the $a'_\sigma$ orbital, whose contour plot is given in Figure 8d, is only slightly perturbed.

The valence orbitals of the dithiocarbamate ligand were obtained from extended Hückel calculations on the simplified model, $S_2CH^-$. Although all calculations were done with $S_2CH^-$, we have verified that $S_2CH^-$ and $S_2CNH_2^-$ have very similar valence orbitals. The three highest occupied valence orbitals are $a_1$, $a_2$, and $b_2$. The $a_2$ orbital is the out-of-phase combination of the p$\pi$ orbitals on the sulfur atoms. The $a_1$ and $b_2$ orbitals are, respectively, in-phase and out-of-phase combinations of the lone-pair orbitals on the sulfur atoms. These two orbitals lie in the plane of the $S_2CH^-$ ligand; contour plots are shown in Figure 9. The crucial orbital is the $b_2$ orbital. It has the proper local symmetry to interact with the $a'_\pi$ orbital of the ($\eta$-$C_5H_5)_2ZrCl^+$ fragment. By matching the nodal planes of the two frontier fragment orbitals, $a'_\pi$ (Figure 8c) and $b_2$ (Figure 9a), one obtains a geometry that is close to the experimental structure. This geometry allows, in addition, nice overlap between the $a'_\sigma$ orbital of the ($\eta$-$C_5H_5)_2ZrCl^+$ fragment (Figure 8d) and the $a_1$ orbital of the $S_2CH^-$ ligand (Figure 9b). These interactions are summarized in the interaction diagram of Figure 10; the $a_1$ and $b_2$ orbitals of $S_2CH^-$ are both stabilized by the empty orbitals of the ($\eta$-$C_5H_5)_2ZrCl^+$ fragment. The $S_2CH^-$ $a_2$ orbital behaves differently. It is destabilized by occupied orbitals on chlorine and the $\eta$-$C_5H_5$ rings. In fact, the $a_2$ orbital becomes the HOMO of the complex.

With use of extended Hückel calculations,[64] the geometry of ($\eta$-$C_5H_5)_2ZrCl(S_2CH)$ **5** was optimized as a function of the angles $\alpha$ and $\omega$, which define the orientation of the Zr–Cl and Zr–C vectors with respect to the $C_2$ axis of the ($\eta$-$C_5H_5)_2Zr$ fragment. $C_s$ symmetry was assumed, and other structural parameters were fixed at the values given in the Appendix. The optimum structure was found for $\alpha = 68.5°$ and $\omega = 39°$, which puts the Zr–$S_1$ bond 7° off the $C_2$ axis in the direction shown in **5**. The calculated values of $\alpha$ and $\omega$ agree well with the observed values of $\alpha = 66.3°$ and $\omega = 38.9°$. Also in agreement with the observed structure are calculated bond orders for Zr–$S_1$ (0.446) and Zr–$S_2$ (0.431), obtained by assuming equal Zr–S bond lengths. This is an indication that Zr–$S_1$ should be shorter than Zr–$S_2$.

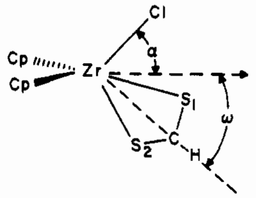

**5**

The geometry of ($\eta$-$C_5H_5)_2ZrCl(S_2CNR_2)$ complexes is not surprising in view of the structure of the isoelectronic molecules ($\eta$-$C_5H_5)_2Nb(CH_3)(C_2H_4)$[65] and ($\eta$-$C_5H_5)_2Zr(COCH_3)$.[10] For instance, ($\eta$-$C_5H_5)_2Nb(CH_3)(C_2H_4)$ may be regarded as a $d^2$ complex that contains a neutral olefin or a $d^0$ complex that contains a doubly negative olefin. No matter how the electrons are counted, the major bonding interaction involves the metal fragment $a'_\pi$ orbital (filled if $d^2$, empty if $d^0$) with the olefin $\pi^*$ orbital (empty if the metal is $d^2$, filled if the metal is $d^0$). The olefin $\pi^*$ orbital takes the place of the $S_2CH^-$ $b_2$ orbital in ($\eta$-$C_5H_5)_2ZrCl(S_2CH)$; indeed the spatial analogy between these two orbitals is evident from the contour plot in Figure 9, as is the analogy between the olefin $\pi$ and the $S_2CH^-$ $a_1$ orbitals. A similar orbital analysis for ($\eta$-$C_5H_5)_2Zr(CH_3)(COCH_3)$ has been carried out by Hofmann and coworkers.[66]

**B. Metal-Centered Rearrangements.** Extended Hückel calculations on the transition states of the digonal twist and chloride migration mechanisms, mechanisms c and d in Figure 6, indicate that these nondissociative rearrangement pathways can be ruled out on the basis of the very high energy of the transition states. Both steric and electronic effects cooperate in producing the high barriers. The digonal twist transition state, obtained by rotating the $S_2CH^-$ ligand by 90° about its twofold axis, has very close contacts between the S atoms and the cyclopentadienyl C atoms. In addition, the ($\eta$-$C_5H_5)_2ZrCl^+$ fragment has no low-lying empty orbitals that

---

(64) (a) Hoffmann, R. *J. Chem. Phys.* **1963**, *39*, 1397. (b) Hoffmann, R.; Lipscomb, W. N. *Ibid.* **1962**, *36*, 2179; **1962**, *37*, 2872.

(65) Guggenberger, L. J.; Meakin, P.; Tebbe, F. N. *J. Am. Chem. Soc.* **1974**, *96*, 5420.

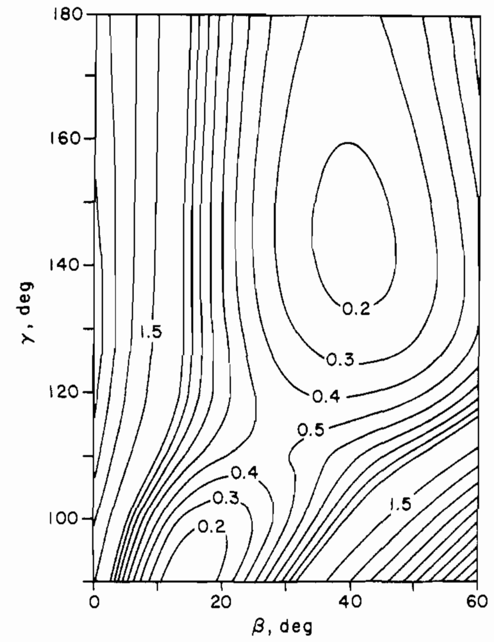

**Figure 11.** A two-dimensional section of the potential energy surface for $(\eta\text{-}C_5H_5)_2ZrCl(S_2CH)$. $E(\alpha,\beta,\gamma)$ is plotted for $\alpha = 60°$. The contours between 0.2 and 1.0 eV are at intervals of 0.1 eV; those above 1.0 eV are at intervals of 0.5 eV.

can interact with the $S_2CH^-$ HOMO, which is now of $b_1$ symmetry, **6**. The barrier to digonal twisting depends on the (centroid $C_5H_5$)–Zr–(centroid $C_5H_5$) angle, but the minimum barrier was found to be 70 kcal/mol. An even higher barrier (95 kcal/mol) was calculated for the chloride migration mechanism. The trigonal-bipyramidal transition state is destabilized by very short cyclopentadienyl C···Cl and C···S contacts and also by unfavorable electronic effects. The e′ metal orbitals do not interact strongly with the e′ symmetry-adapted combination of ligand orbitals **7** because the metal d orbitals have two nodes while the ligand combinations have one node.[67] Consequently, bonding in the equatorial plane is weak.

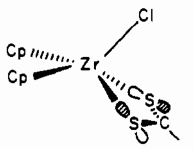

**6**

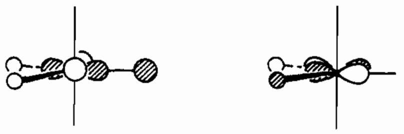

**7**

The ease of Zr–S bond rupture in $(\eta\text{-}C_5H_5)_2ZrCl(S_2CH)$ was investigated by calculating the potential energy surface for interconversion of the five-coordinate, chelated isomer and the four-coordinate, ring-opened isomer. The energy was calculated as a function of the angular parameters β and γ for a series of values of the angle α; α, β, and γ are defined in **8**. In order to reduce the number of degrees of freedom, we kept the remaining angles and the bond distances constant at the values given in the Appendix. A two-dimensional section of the potential energy surface, $E(\alpha,\beta,\gamma)$ for $\alpha = 60°$, is presented in Figure 11. Two minima are apparent: one for the chelated structure ($\beta = 15°$, $\gamma = 90°$); the other for a ring-opened structure ($\beta = 42°$, $\gamma = 150°$, corresponding to a Zr···$S_2$ distance of 4.8 Å). The surface is especially flat in the region of the second minimum, and the geometry of the ring-opened structure is not precisely determined.

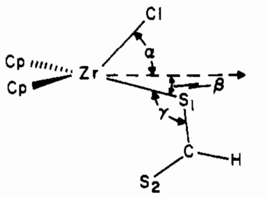

**8**

The positions of the Cl atom and the $S_2CH^-$ ligand are strongly correlated. The chelated structure is stable only for large values of α, while the ring-opened structure becomes increasingly stable as α decreases. Analysis of two-dimensional sections of the potential energy surface as a function of α allows the optimum geometry of the ring-opened structure to be located around $\alpha = 45°$, $\beta = 50°$, $\gamma = 150°$. Again, the location of the minimum is approximate because the surface is very flat. For $\alpha = 45°$, there is no longer a minimum for the chelated structure. The Cl–Zr–$S_1$ angle in the ring-opened structure (95°) compares nicely with typical L–M–L angles in $d^0$ $(\eta\text{-}C_5H_5)_2ML_2$ complexes (94–97°).[5]

The most striking feature of the ring-opened structure is the very large angle (150°) at sulfur atom $S_1$. Ordinarily, a dicoordinated sulfur atom prefers a more acute angle, usually around 90°. A similar distortion has been noted in $(\eta\text{-}C_5H_5)_2ZrCl[CH_2P(C_6H_5)_2]$ (**9**) where the observed angle at the carbon atom is 130°.[63] Two reasons are suggested for such a large angle. First, as the angle at $S_1$ becomes more obtuse, the lone pair on $S_1$ has more p character and less s character; this leads to an optimum match between the $S_1$ component of the ligand $b_2$ orbital and the $a'_\pi$ orbital of the $(\eta\text{-}C_5H_5)_2ZrCl^+$ fragment, **10**. Second, a large angle at $S_1$ avoids a strong antibonding overlap between $a'_\pi$ and the $S_2$ component of the ligand $b_2$ orbital. The total Zr–$S_2$ bond order in **10** is negative, although small (−0.007). In the chelated structure, the interaction of the $a'_\pi$ and $b_2$ orbitals is in phase at both $S_1$ and $S_2$, **11**. The difference in the Zr–$S_2$ interaction (antibonding in **10**, bonding in **11**) is accompanied by a change in the Zr–$S_1$ bond type (π type in **10**, σ type in **11**). The antibonding interaction between Zr and $S_2$ is relieved in the trans conformer **12**; however, **12** was found to be isoenergetic with the cis conformer **8**.

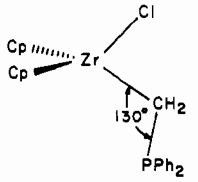

**9**

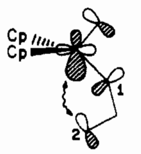

**10**

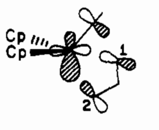

**11**

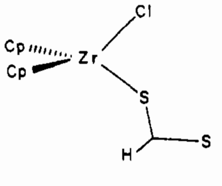

**12**

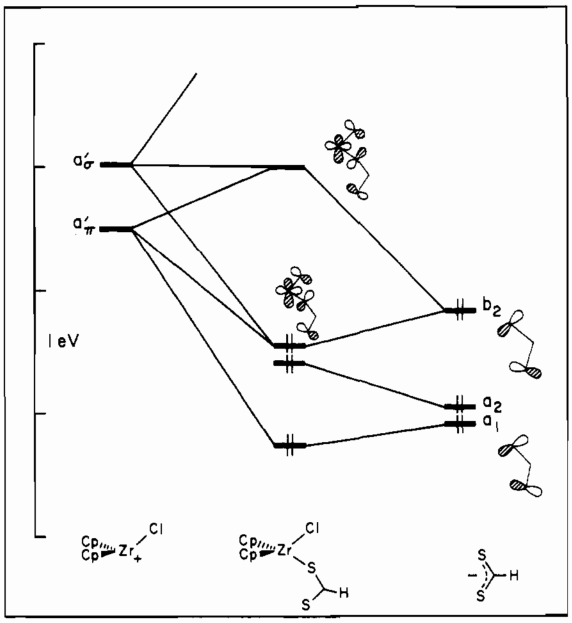

**Figure 12.** Interaction diagram for the ring-opened isomer of ($\eta$-$C_5H_5)_2ZrCl(S_2CH)$.

An interaction diagram for the ring-opened isomer is shown in Figure 12. Interaction between the $a'_\pi$ and $b_2$ orbitals is relatively weak since the interaction involves a $\pi$-type bond. The $b_2$ orbital is weakly stabilized, and the $a'_\pi$ orbital is only weakly destabilized. A rather small HOMO-LUMO gap results (1.6 eV), which suggests that the ring-opened isomer may be susceptible to reduction.[68] Facile reduction of ($\eta$-$C_5H_5)_2ZrCl[CH_2P(C_6H_5)_2]$ has been reported.[63]

The activation energy for interconversion of the chelated and ring-opened isomers of ($\eta$-$C_5H_5)_2ZrCl(S_2CH)$ is certainly very small. When $\alpha$ is kept constant at 60° (cf. Figure 11), our calculation gives an activation energy of less than 10 kcal/mol. Allowing $\alpha$ to vary simultaneously with $\beta$ and $\gamma$ decreases the activation energy. In fact, there is a pathway leading from the optimized chelated structure to the optimized ring-opened structure with no activation energy if $\alpha$, $\beta$, and $\gamma$ are varied synchronously. (Our optimized ring-opened structure is more stable than the optimized chelated structure by 10 kcal/mol.) This absence of activation energy is probably due to the known weakness of the extended Hückel method in dealing with changes in bond length. No changes in the relative energies of the chelated and ring-opened isomers were found when the $S_2CH^-$ ligand was replaced by $S_2CNH_2^-$. Despite the above-mentioned weakness of the extended Hückel method, one can conclude that interconversion of the chelated and ring-opened isomers should be a facile equilibrium process.

**Table IX.** Parameters for Extended Hückel Calculations

| atom | orbital | $\zeta$ | $H_{ii}$, eV |
|---|---|---|---|
| Zr | 5s | 1.9 | −10.15 |
| | 5p | 1.85 | −6.85 |
| | 4d | 4.08 (0.6401)[a]<br>1.64 (0.5516) | −12.1 |
| Cl | 3s | 2.033 | −26.3 |
| | 3p | 2.033 | −14.2 |
| S | 3s | 1.817 | −20.0 |
| | 3p | 1.817 | −13.3 |

[a] Coefficients of the double-$\zeta$ 4d functions are given in parentheses.

One way to tune this equilibrium is to vary the nature of the ligand L on the ($\eta$-$C_5H_5)_2ZrL$ fragment. We have seen previously that $\pi$-donor L groups destabilize the fragment $a'_\pi$ orbital (cf. Figure 7). This leads to a decrease in the $a'_\pi$–$b_2$ ($S_2CH^-$) interaction, which is so important in stabilizing the chelated structure (cf. Figure 10). A calculation on ($\eta$-$C_5H_5)_2ZrH(S_2CH)$ shows that the chelated structure is relatively more stable (i.e. relative to the ring-opened structure) for ($\eta$-$C_5H_5)_2ZrH(S_2CH)$ than for ($\eta$-$C_5H_5)_2ZrCl(S_2CH)$. A related experimental result,[62] in agreement with this picture of the bonding, concerns the fluxionality of ($\eta$-$C_5H_5)_2ZrL[(CH_2)P(CH_2)(CH_3)_2]$ (L = H or Cl) (**13**). The chloride complex undergoes exchange of the methylene groups at ~50 °C, by a proposed mechanism that involves formation of the ring-opened isomer **14**, while the hydride derivative is stereochemically rigid up to 85 °C. For ($\eta$-$C_5H_5)_2ZrCl[CH_2P(C_6H_5)_2]$, the ring-opened isomer **9** is the stable structure.[63] In the case of ($\eta$-$C_5H_5)_2ZrL(S_2CNR_2)$ complexes, it appears that Zr–L $\pi$ bonding may not be sufficient to destabilize the chelated isomer; $Cl^-$ is already a good $\pi$ donor. It is possible that a bulky L group may be required to produce a stable monodentate attachment of the dithiocarbamate ligand.

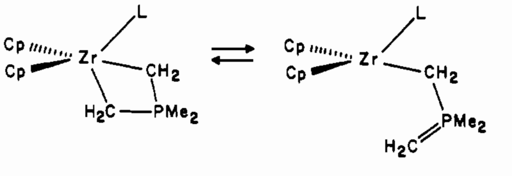

**13** **14**

Finally, we wish to comment on the relative merits of Zr–S bond rupture mechanisms e and f of Figure 6. Zr–S bond rupture by itself does not suffice to exchange the inequivalent dithiocarbamate methyl groups; bond rupture must be followed by rotation about one or more bonds. Rotation about the Zr–S bond is sterically hindered despite the large Zr–S–C angle in the ring-opened structure. Rotation about the C–S bond or simultaneous rotation about the C–S and Zr–S bonds is more likely. Ab initio calculations have given a barrier of 12 kcal/mol for rotation about the C—S single bond in dithioformic acid HS—CH═S.[69] However, a higher barrier can be expected in ($\eta$-$C_5H_5)_2ZrCl(S_2CNR_2)$ complexes because of close contact in the transition state between an $\eta$-$C_5H_5$ ligand and the $NR_2$ group. Rotation about the C⎓N bond (mechanism f) is free of steric hindrance, and it is this mechanism, or mechanism g, that is favored by the experimental data.

**Acknowledgment.** We wish to thank Greta Chang for assistance with the synthetic work and P. Hofmann for communicating results prior to publication. M.E.S. thanks Dow Chemical Co. for a fellowship. The X-ray diffractometer and 300-MHz NMR spectrometer used in this research were obtained with support from the National Science Foundation Instrumentation Program.

## Appendix

The extended Hückel calculations were performed with the ICON 8 program using the weighted $H_{ij}$ formula[70] and standard parameters for carbon and hydrogen. The parameters employed for Zr, Cl, and S are given in Table IX. The following

---

(66) Hofmann, P., private communication.

(67) (a) Hoffmann, R.; Howell, J. M.; Muetterties, E. L. *J. Am. Chem. Soc.* **1972**, *94*, 3047. (b) Rossi, A. R.; Hoffmann, R. *Inorg. Chem.* **1975**, *14*, 365.

(68) This point is analyzed in detail by Hofmann et al. in calculations on ($\eta$-$C_5H_5)_2ZrCl[CH_2P(C_6H_5)_2]$: Hofmann, P.; Stauffert, P.; Schore, N. E. *Chem. Ber.* **1982**, *115*, 2153.

(69) (a) Auberg, E.; Samdal, S.; Seip, H. M. *J. Mol. Struct.* **1979**, *57*, 95. (b) Bak, B.; Neilsen, O.; Svanholt, H. *J. Mol. Spectrosc.* **1979**, *75*, 134.

(70) Ammeter, J. H.; Burgi, H.-B.; Thibeault, J. C.; Hoffmann, R. *J. Am. Chem. Soc.* **1978**, *100*, 3686.

distances and angles were kept fixed: Zr–Cl = 2.55 Å, Zr–S = 2.72 Å, Zr–(centroid of $C_5H_5$) = 2.22 Å, cyclopentadienyl C–C = 1.40 Å, C–H = 1.08 Å, C–S = 1.71 Å, S–C–S = 115.7°. The angle between the normals to the planes of the two $\eta$-$C_5H_5$ rings was set equal to 138°.

**Registry No.** $(\eta\text{-}C_5H_5)_2ZrCl[S_2CN(C_2H_5)_2]$, 66943-46-2; $(\eta\text{-}C_5H_5)_2ZrCl[S_2CN(CH_3)_2]$, 66943-45-1.

**Supplementary Material Available:** A listing of structure factor amplitudes for $(\eta\text{-}C_5H_5)_2ZrCl[S_2CN(C_2H_5)_2]$ (10 pages). Ordering information is given on any current masthead page.

---

Contribution from the Department of Chemistry,
Texas A&M University, College Station, Texas 77843

# Comparison of the Eight-Coordinate Structures of $d^1$ $TaCl_4(dmpe)_2$ and $d^0$ $TaCl_4(dmpe)_2^+$

F. ALBERT COTTON,* LARRY R. FALVELLO, and ROBERT C. NAJJAR

*Received June 9, 1982*

The structures of $[P(CH_3)_4][TaCl_4(dmpe)_2]_3Cl_4\cdot4(CH_3)_2S$ (**1**) and $TaCl_4(dmpe)_2$ (**2**) have been determined by X-ray crystallography to examine the structural effects of adding one d electron to the $d^0$ cation $TaCl_4(dmpe)_2^+$. The $TaCl_4(dmpe)_2^+$ ion has a structure of the dodecahedral type previously found for similar $Ta^V$ complexes; the bond lengths and angles are as follows: Ta–Cl, 2.430 (3) Å; Ta–P, 2.691 (5) Å; P–Ta–P, 72.1 (2)°; Cl–Ta–Cl, 145.4 (2)°. The neutral molecule, **2**, has a structure that is approximately square antiprismatic with the following bond lengths: Ta–Cl, 2.505 [3] Å; Ta–P, 2.653 [2] Å. Compound **1** forms cubic crystals in the space group $I\bar{4}3m$ with a unit cell edge of 16.726 (7) Å, a cell volume of 4679 (6) Å$^3$, and $Z = 2$. The Ta atoms reside on positions of $\bar{4}2m$ symmetry. Compound **2** forms orthorhombic crystals in the space group $P2_12_12$ with unit cell dimensions $a = 10.765$ (2) Å, $b = 11.297$ (4) Å, $c = 9.595$ (3) Å, $V = 1167$ (3) Å$^3$, and $Z = 2$. The molecules have a crystallographic twofold axis of symmetry.

## Introduction

Coordination number 8 can be considered uncommon only in a relative sense. There are, in fact, many examples of it, and several geometric forms are well-known.[1,2] We are concerned here with a question that is simple in concept but rarely answerable experimentally: What will be the effect of adding one electron to a given eight-coordinate species on its structure? We were led to our particular study of this question in the following way.

In the course of preparing the new compound[3] $Ta_2Cl_6(dmpe)_2$, where dmpe represents $Me_2PCH_2CH_2PMe_2$, we isolated a very small amount of a beautifully crystalline yellow compound, **1**. A crystallographic study of this compound showed that it contains the $[TaCl_4(dmpe)_2]^+$ ion, which has a dodecahedral structure of the type previously reported[1] for several $[MX_4(diars)_2]^+$ ions with M = Nb and Ta, X = Cl and Br, and diars = $o$-$(Me_2As)_2C_6H_4$. In these structures the *diars* ligands span the positions marked X in Figure 1 and the four halide ions occupy the Y positions. The symmetries of these molecules are essentially $D_{2d}$ although this is not crystallographically rigorous. In our $[TaCl_4(dmpe)_2]^+$ ion crystallographic $\bar{4}2m$ symmetry of the $TaCl_4P_4$ core was found.

Since the neutral, homologous compound $TaCl_4(dmpe)_2$ had already been reported,[4] we recognized an opportunity to see what effects the presence of one d electron would have on the structure. It had previously been claimed[5] from powder diffraction work that $NbCl_4(diars)_2$ retained the dodecahedral geometry of the $[NbCl_4(diars)_2]^+$ ion, but no quantitative information about bond lengths or bond angles was likely to be obtainable for $NbCl_4(diars)_2$ since it was reported[5] to be impossible to find a solvent from which to recrystallize it.

We have been able to obtain the detailed crystal structure of $TaCl_4(dmpe)_2$ (**2**) and find that the geometry is not dodecahedral but square antiprismatic.

## Experimental Section

The solvents, $CH_2Cl_2$ and THF, were dried over $P_2O_5$ and potassium benzophenone ketyl, respectively. The compound $TaCl_4(dmpe)_2$ (**2**) was prepared by the literature method[4] with bis(dimethylphosphino)ethane, dmpe, purchased from Strem Chemicals. All materials were handled under argon with use of Schlenk and vacuum-line techniques. $Ta_2Cl_6(SMe_2)_3$ was prepared as described previously.[6]

**Preparation of $[P(CH_3)_4][TaCl_4(dmpe)_2]_3Cl_4\cdot4(CH_3)_2S$ (1).** An addition funnel was charged with 4 equiv[7] of dmpe (0.45 mL, 2.70 mmol) followed by 10 mL of $CH_2Cl_2$ and attached to a flask containing $Ta_2Cl_6(SMe_2)_3$ (0.5 g, 0.66 mmol) dissolved in 20 mL of $CH_2Cl_2$. The contents of the addition funnel were added to the flask slowly, and the solution was allowed to stand at 25 °C for 24 h, yielding a yellow-brown solution and a red precipitate. The solvent was removed by vacuum distillation, and the resulting orange-brown solid was extracted with hexane (2 × 10 mL) to remove excess dmpe. The solid was redissolved in $CH_2Cl_2$ and filtered through a Celite pad, leaving the insoluble red material behind. After the solution had stood 5 days at 25 °C, a deep yellow solution over a large amount of red solid[5] was obtained. Intermixed with the red solid were cubic yellow crystals of **1** of suitable quality for X-ray analysis, in ca. 5% yield. Crystals of **1** were mildly moisture sensitive (decomposition in moist air in <10 h).

**X-ray Crystallography of Compound 1.** Geometric and intensity data were obtained from a crystal of dimensions 0.30 × 0.30 × 0.25 mm. The crystal was sealed inside a glass capillary tube and mounted on an automated four-circle diffractometer (Enraf-Nonius CAD-4) equipped with a Mo X-ray tube ($\lambda\bar{\alpha}$ = 0.710 73 Å) and a graphite monochromator.

Unit cell dimensions and the orientation matrix were given by a least-squares fit of these parameters to the goniometer positions of 25 well-centered reflections in the range 29.8° < $2\theta$ < 38.5°. The

---

(1) Kepert, D. L. *Prog. Inorg. Chem.* **1978**, *24*, 179.
(2) Burdett, J. K.; Hoffmann, R.; Fay, R. C. *Inorg. Chem.* **1978**, *17*, 2553.
(3) Cotton, F. A.; Falvello, L. R.; Najjar, R. C. *Inorg. Chem.* **1983**, *22*, 375.
(4) Datta, S.; Wreford, S. S. *Inorg. Chem.* **1977**, *16*, 1134.
(5) Clark, R. J. H.; Kepert, D. L.; Lewis, J.; Nyholm, R. S. *J. Chem. Soc.* **1965**, 2865.
(6) Cotton, F. A.; Najjar, R. C. *Inorg. Chem.* **1981**, *20*, 2716.
(7) When less dmpe was used, a complex mixture of products that could not be separated was obtained.

0020-1669/83/1322-0770$01.50/0